HUGHES

SANTA BARBARA RESEARCH CENTER
a subsidiary

MAPPING PHOTOPOLARIMETER SPECTROMETER INSTRUMENT FEASIBILITY STUDY FOR FUTURE PLANETARY FLIGHT MISSIONS

FINAL REPORT

PREPARED FOR
**NATIONAL AERONAUTICS AND SPACE ADMINISTRATION
GODDARD SPACE FLIGHT CENTER
INSTITUTE FOR SPACE STUDIES**
2880 Broadway, New York, NY 10025

CONTRACT NO. NAS5-30531
SBRC REF. 90-1045
OCTOBER 1990

SANTA BARBARA RESEARCH CENTER

A Subsidiary of Hughes Aircraft Company

75 COROMAR DRIVE, GOLETA, CALIFORNIA

MAPPING PHOTOPOLARIMETER SPECTROMETER INSTRUMENT FEASIBILITY STUDY FOR FUTURE PLANETARY FLIGHT MISSIONS

FINAL REPORT

Prepared For

NATIONAL AERONAUTICS AND SPACE ADMINISTRATION
GODDARD SPACE FLIGHT CENTER
INSTITUTE FOR SPACE STUDIES
2880 Broadway, New York, NY 10025

Contract No. NAS5-30531
SBRC Reference No. 90-1045

October 1990

ABSTRACT

This report summarizes evaluations directed towards defining optimal instrumentation for performing planetary polarization measurements from a spacecraft platform. An overview of the science rationale for polarimetric measurements is given to point out the importance of such measurements for future studies and exploration of the outer planets. The key instrument features required to perform the needed measurements are discussed and applied to the requirements for the Cassini mission to Saturn. The resultant conceptual design of a spectro-polarimeter photometer for Cassini is described in detail.

CONTENTS

ILLUSTRATIONS

TABLES

INTRODUCTION

This final report for the Mapping Photopolarimeter Spectrometer (MPS) Instrument Feasibility study for future planetary flight missions summarizes evaluations directed towards defining optimal instrumentation for performing planetary polarization measurements from a spacecraft platform. In Section 1 a brief overview of the basic science rationale for polarimetric measurements is given to point out the importance of such measurements for future studies and exploration of the outer planets. This is followed in Section 2 by a discussion of the key instrument features required to perform the needed measurements. In Section 3 these approaches are refined for and applied to the needs of the Cassini mission to Titan and Saturn as a conceptual design for the Spectro-Polarimeter/Photometer (SPP) instrument.

Section 1
RATIONALE FOR POLARIMETRIC MEASUREMENTS

Sunlight reflected by planetary objects is in general polarized and contains embedded information as to the innate characteristics of the compositional, microphysical, and large-scale structure of the illuminated object. Some of this information is accessible to standard modeling techniques which utilize the intensity (only) variations with wavelength and with viewing geometry. These standard methods are often able to infer important compositional and structural information and provide the bulk of our current knowledge about planetary objects. Additional detailed information (e.g., planetary cloud composition, cloud microphysical structure, microstructure of solid-body surfaces) is not readily obtainable from modeling efforts that are limited to analyzing only light intensity variations, but this information is fully accessible to radiative modeling methods that are able to interpret the polarization signature of the reflected light. The key observational parameters that most strongly constrain the utility and effective information content of polarization measurements are: (1) the phase angle range over which the polarization measurements can be obtained, (2) the spectral range and resolution of the measurements, and (3) the spatial resolution and geographic context of the observations.

For a given physical quantity, say, particle size or refractive index, its polarization signature is displayed across the full phase angle range (0 - 180°) as illustrated in Figure 1-1. For an inner planets such as Venus, essentially the full phase angle range is accessible for ground-based ob-servations. Unfortunately, for the outer planets, their satellites, and neighboring asteroids, the ac-cessible phase angle range for ground-based observations is very severely restricted - it is less than 12° for Jupiter and less than 2° for Neptune. Hence, space mission observations offer the
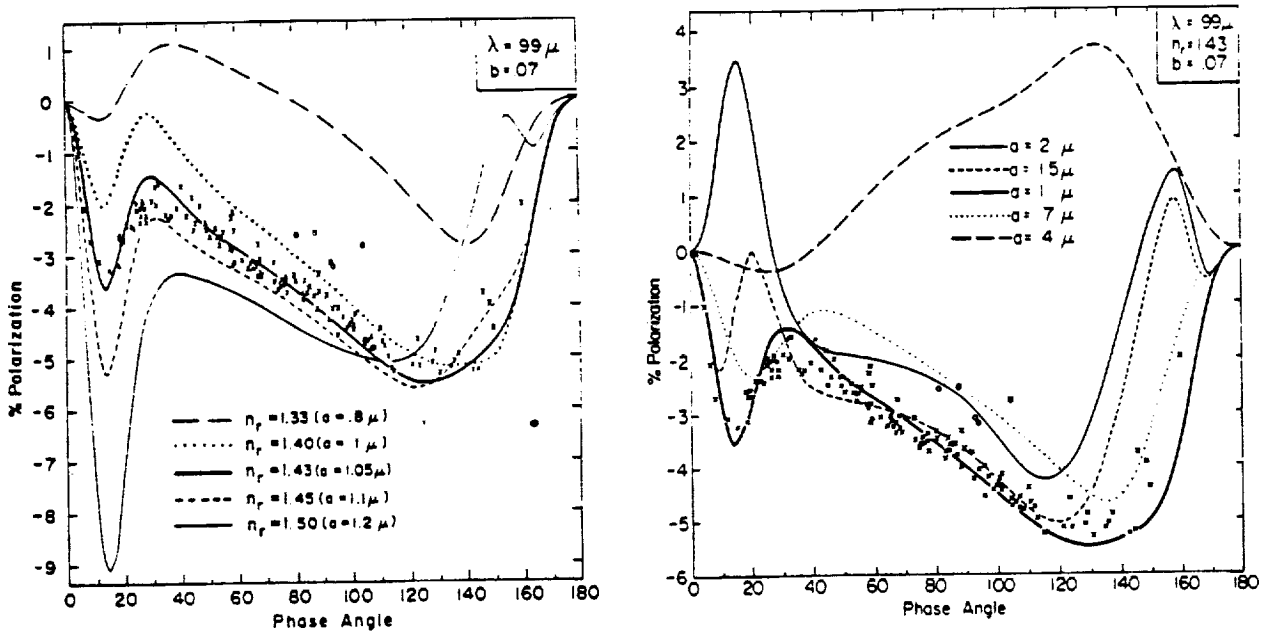
Figure 1-1. **Earth-based Observations of the Polarization of Sunlight Reflected by Venus in the Near Infrared.** *The observations, which are the same in both halves of the figure, were made by Coffeen and Gehrels with an intermediate bandpass filter centered at λ = 0.99 μm. The theoretical curves on the left show the sensitivity of the polarization to the particle refractive index n_r, the mean particle radius a being selected in each case to yield the closest agreement with the observations in the ultraviolet, visible, and infrared. The theoretical curves on the right show the sensitivity of the polarization to the mean particle size a for the particular value of the refractive index $n_r = 1.43$.*

only opportunity for obtaining an adequate phase angle range for the study of polarization in the atmospheres of the outer planets.

Additional polarimetric information is found in the spectral variability of polarization features over the full range of the solar spectrum. This wavelength dependence is a sensitive tool for discriminating: (1) cloud particle size distributions - particularly for size ranges that are the same order of magnitude as the observation wavelength, (2) cloud particle composition in terms of its refractive index spectral signature, and (3) cloud particle number density and cloud-top pressure using the strong wavelength dependence ($\propto \lambda^{-4}$) of Rayleigh scattering.

The rich information content of polarized light, and the retrieval of this information from remote sensing measurements, is best illustrated for the case of Venus. Ground based polarization measurements spanning the spectrum from ~ 0.35 - 0.95 μm were analyzed by Hansen and Hovenier (J. Atmos. Sci. 31, 1137, 1974) to extract precise limits for the cloud particle refractive index (and its spectral dispersion), the cloud particle shape and size distribution (including its variance), and the cloud-top pressure at optical depth (τ) unity. The results of this analysis were sufficiently restrictive to rule out all previously suggested cloud composition candidates except

for concentrated (75%) sulfuric acid. It is fair to note that the success of this illustrative example was aided by the fortuitous combination of spherical cloud particles comprising the cloud-tops of the Venus atmosphere, a nearly complete range of phase angle coverage, and the availability of an exact theory (and computing resources) to calculate the single and multiple scattering contributions from a polydispersion of spherical cloud particles.

Polarimetric analyses to retrieve detailed cloud microphysical information for outer planet atmospheres have met with more limited success primarily because there is a lack of comprehensive observational data beyond the small phase angle range that is accessible to ground-based observations. While more extensive phase angle coverage was available from the Pioneer and Voyager missions, the measurements were limited by the flyby nature of the missions, the relatively small spectral coverage of the polarimeters, and low accuracy and instrumental problems of the Voyager polarimeters. The Galileo mission which will be comprised of many orbits around Jupiter offers much greater opportunity for detailed polarimetry of Jupiter with the Photopolarimeter/Radiometer instrument. The planned Cassini mission to Saturn offers similar opportunities for the Saturnian planetary system.

The current lack of exact mathematical theory (the equivalent of Mie theory for spherical particles to compute the single scattering phase matrix) for arbitrarily shaped particles does <u>not</u> pose a significant obstacle for theoretical modeling of multiple scattering processes and extracting useful information from polarization measurements. "Exact" single scattering phase functions have been computed for for a number of non-spherical particle shapes, e.g., spheroids (Asano and Sato, Appl. Opt. <u>19</u>, 962, 1980), and infinite cylinders (Liou, J. Atmos. Sci. <u>29</u>, 524, 1972). Moreover, the single scattering phase matrix (which is the basic input to radiative transfer models) can also be measured directly for different types of laboratory generated NH_3 and H_2O ice clouds (e.g., Holmes et al., Bull. Amer. Astron. Soc. <u>12</u>, 705, 1980). Also, since polarization properties scale according to the size parameter $2\pi r/\lambda$ (where r is the particle radius), microwave analog methods (e.g., Greenberg et al., J. Appl. Phys. <u>32</u>, 333, 1961), or photometric and laser scattering methods (e.g., Holland and Gange, Appl. Opt. <u>9</u>, 1113, 1970) can be used to obtain single scattering phase matrices for realistic physical models.

Good spatial resolution with accurate mapping of observational data is also important for effective interpretation of polarimetric measurements and their placement into proper geographical context to permit meaningful comparison with other spatially resolved quantities. Scarcely any object in the solar system is sufficiently homogeneous as not to require spatially resolved measurements.

A precise mathematical theory of light scattering by solid surfaces is not necessary to make useful empirical interpretation of polarization measurements. By this process, Lyot (Ann. Obs. Meudon 8, Part 1, 1929) was able to deduce that the lunar surface was covered almost entirely by a powdery material resembling volcanic ash long before direct verification became possible. The key parameters defining the polarization-phase curves typical of most asteroids are shown in Figure 1-2 along with an illustration of the relationship between the geometric albedo and the minimum polarization P_{min} for selected astronomical bodies (Bowell and Zellner, in *Planets, Stars and Nebulae Studied with Photopolarimetry*, ed. T. Gehrels, 1974). Wolff (Icarus 44, 780, 1980) has provided a theoretical basis for interpreting the polarization from solid surfaces in terms of the refractive index of the surface material. This, together with the wavelength dependence of the polarization, provides a means for determining the gross composition of the surface.
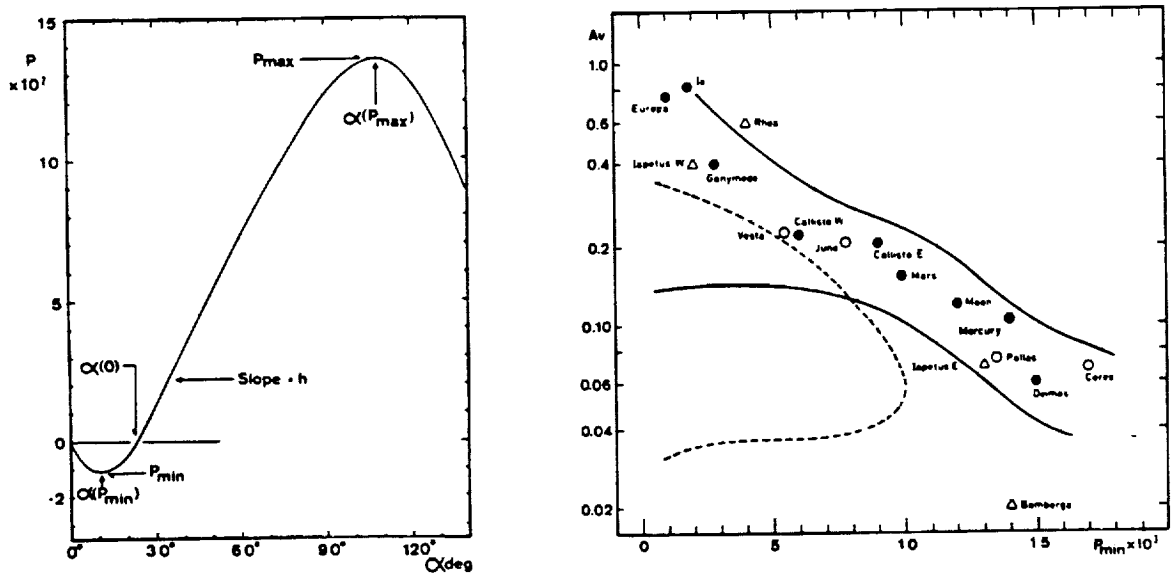
Figure 1-2. **Definition of Parameters for Polarization-phase Curves.** *The right hand panel gives the geometric albedo at 0.55 µm versus P_{min} for selected astronomical bodies (after Bowell and Zellner, 1974).*

It is clear that polarized light reflected from planetary objects contains a rich assortment of detailed information regarding the microphysical, compositional, and large-scale structure of the illuminated objects. While the retrieval of this information from remote sensing measurements of polarized light may require considerable theoretical effort, the necessary tools are available.

The key requirement for extracting the information contained in polarized light is comprehensive phase angle coverage, with adequate spectral and spatial resolution. It is appropriate to note here that it is adequate to measure only the linear polarization characteristics as the circular polarization component is negligible for virtually all scenes of interest.

Section 2
CANDIDATE INSTRUMENT CONCEPTS

To meet the measurement requirements outlined above, a wide range of polarimetric measurement methods were evaluated for their suitability. The various approaches are reviewed here with some discussion of the features of importance. For the polarimeter class found to best satisfy the requirements, a modeling of the prime characteristics is included.

2.1 CLASSIFICATION OF POLARIMETRIC MEASUREMENT METHODS

Of the various types of optical polarimeters used to measure linear polarization, a fundamental difference in approach and design exists between those that: (1) use a beamsplitting (birefringent) analyzer and paired detectors to simultaneously measure orthogonal polarization components of the incident beam; and (2) measure only a single polarization component at several analyzer positions. A Wollaston prism has high polarization separation ($\sim 10^5$) and is typically used as the polarization beamsplitter in two-beam polarimeters. Since the single-beam approach uses only one detector per spatial resolution element, the analyzer can be a dichroic element that transmits one of the linearly polarized components and absorbs the other. In spite of the cross calibration of the detectors required for the two-beam polarimeters, the accuracy of such systems has been demonstrated to be clearly superior to the accuracy of single-beam polarimeters (see for example, D. L. Coffeen, p. 189, in *Planets, Stars and Nebulae Studied with Photopolarimetry*, ed. T. Gehrels, 1974). The principal reason for this superiority is the "false polarization" that can result when time sequential polarization component measurements are made. Such false polarization can occur whenever scene viewing conditions change between measurement of orthogonal polarization components (see later subsection where this effect is quantified).

Two-Beam Area Array Approaches

Where a two-beam measurement technique is used and multiple spatial elements are to be detected simultaneously, i.e., by "area imaging", a further problem exists that is not present with a properly designed single instantaneous field of view (IFOV) instrument. (Such proper design requires that the IFOV be determined prior to the polarization separation.) This problem is that exact alignment of all equivalent detector pairs is required to achieve high accuracy polarimetry, and this is essentially impossible to assure unless the "pixels" are defined prior to polarization separation and the pixels are reimaged onto oversized detectors of uniform response. The over-sized detector elements are necessary to accommodate any misalignment of equivalent detectors. It is clear that with this approach only a fraction of the scene radiance within the overall field of view is utilized, i.e., the pixel-to-pixel spacing must be significantly greater than the "effective"

pixel size. This situation may not be acceptable for spatial characterization of the scene. A further disadvantage of this approach is that spectral measurements typically would need to be done in time sequential fashion.

A modification of the above area imaging approach is the use of one array dimension for spatial definition and the other for spectral definition with areal coverage being provided by a scanning method, e.g., by spacecraft scan platform motion. The use of a multiple pixel entrance "slit" with the scene spectral content angularly spread in the exit plane of a dispersive spectrometer would be such an approach. For high polarimetric accuracy the same basic restrictions would apply as indicated above. Basically, since the pixels along the entrance "slit" must be defined there for acceptable polarimetric accuracy, the pixels cannot be contiguous. The result is a low spatial sampling efficiency in that dimension. (A staggered arrangement of IFOVs, e.g., a bilinear arrangement, at the entrance "slit" could be used to increase the effective sampling density, but this approach would reduce and complicate accessibility in the spectral dimension.)

Another two-beam area array(s) approach consists of a modification to the wedge filter spectrometer concept to convert it to a polarimeter. In this approach a wedge filter is positioned at the prime focus of the polarimeter telescope with the flux transmitted by the wedge filter being separated into orthogonally polarized beams and relayed onto two area arrays. (The wedge filter is a multilayer bandpass filter with the center wavelength varying spatially in one dimension, i.e., with layer thicknesses graded in thickness in one direction.) Again the necessity of spatial definition at the prime focus as in the previously described methods applies. However, while simultaneous spatial/spectral measurements are collected with this method, a complete spectral data set for a specific pixel can be obtained only when spatial scanning occurs in the spectral direction. In contrast, with the dispersive spectrometer approach a full set of spatially registered spectral data is obtained without any scanning being required. Thus, the dispersive spectrometer approach is superior for a polarimeter that does not have any inherent spatial scan capability, such as is usually the case with scan-platform-mounted instruments.

Single-Beam Area Array Approaches

All single-beam approaches have in common the inherent susceptibility to false polarization since typical "imaging" polarimeter concepts typically can not ensure exact registration during sequential polarization component measurements. Exceptions to this would be designs based on rapid alternation (modulation) between polarization states. The most attractive of these is the piezo-optical modulator based on stress birefringence produced in an isotropic material by acoustic vibrations (J. C. Kemp, JOSA 59, 950 (1969)). Since such modulators typically operate in the tens of kHz range, this would complicate substantially the array read-out and data processing. For ground-based astronomy the use of such high frequency modulation is particularly

useful to reduce substantially the false polarization due to atmospheric seeing and telescope guiding errors (K. Serkowski, p. 135 in Planets, Stars and Nebulae Studied with Photopolarimetry, ed. T. Gehrels, 1974). Furthermore, with these approaches spectral measurements typically would need to be done in time sequential fashion.

Two-Beam, Single IFOV Approaches

The two-beam, single IFOV approaches can be further separated into those providing sequential spectral sampling and those providing simultaneous spectral sampling. Polarimeters such as the Pioneer Venus Orbiter Cloud Photopolarimeter (CPP) and the Galileo Photopolarimeter/Radiometer (PPR) are based on using two detectors, one to detect each of the orthogonally polarized beams exiting a Wollaston prism. In each case, the positioning of a filter/retarder wheel allows measurements at three halfwave retarder azimuths for each of several spectral bands (two retarder positions are required for degree of polarization and polarization azimuth determination with a third position providing detector cross calibration). As a result of careful design, e.g., to avoid false polarization effects, these instruments provide high accuracy measurement of linear polarization (~0.1 to 0.2% for low polarization scenes).

Dichroic filtering after separation of orthogonal polarization components--such as that used on Pioneer 10 and 11 Imaging Photopolarimeter (IPP) instruments--can be used to provide measurements in two or more spectral bands simultaneously. While polarimeter dichroic filtering approaches are viable,where the number of spectral channels is fairly limited, an even greater spectro-polarimetric capability can be achieved by integrating an achromatic halfwave retarder, a Wollaston prism, and two linear arrays into a dispersive spectrometer. With this approach the key elements of the instrument are: 1) an entrance "slit" (a square aperture) that serves as the field stop of an f/5 Cassigrainian telescope; 2) a collimating lens that directs the scene flux through a positionable, superachromatic halfwave retarder and Wollaston prism; 3) a diffraction grating used in an out-of-plane, Czerny-Turner configuration that disperses the two orthogonally polarized beams; and 4) a relay lens that focuses the two beams onto two linear arrays of multiplexed silicon photodiodes made oversized in the non-spectral direction. This approach has been selected as the best choice for the Cassini mission and is evaluated in some detail in Section 3.

Single-Beam, Single-IFOV Approaches

Single-beam polarimeters with a single-IFOV using sequential measurement of orthogonal polarization components clearly are subject to false polarization whenever scene changes occur between component measurements, e.g., due to relative spacecraft-to-scene motions. Thus, Voyager PPS-type instruments are unsuitable for a Cassini type application where polarimetric accuracies of better than about 0.5 percent are required. Similarly, other single-beam, single IFOV approaches that employ a continuously rotating analyzer or retarder are not suitable unless

sufficiently rapid alternation between polarization states is used to avoid false polarization (with the associated problems discussed above). A multiple reflection method (R. M. A. Azzam, Opt. Lett. 10, 309 (1985)) has the potential for high accuracy with no moving parts, but with the disadvantages of requiring large detectors and being poorly suited for simultaneous spectral measurements.

2.2 EFFECTS OF SYSTEM CHARACTERISTICS ON POLARIMETRIC ACCURACY

Critical to the utility of polarimetry in a given application is the polarimetric accuracy of the measurement. In Table 2-1 the effect of a number of system characteristics on polarimetric accuracy is indicated qualitatively. While qualitative, it is useful to review these as they relate to missions to the outer planets.

The desirable features of a telescope design suitable for polarimetry can be easily stated. These include: (1) a symmetrical design, e.g., a Cassigrainian form; (2) small angles of incidence on the mirrors which implies a relatively high f/number, i.e., > f/4; (3) minimization of the number of mirrors in the fore optics, i.e., clearly best kept to two; and (4) coating the telescope mirrors in a well-controlled, symmetrical manner to minimize mirror asymmetries. It is probable that future missions to the outer planets will use high precision scan platforms to provide the pointing for the optical instruments. As a consequence, it is both appropriate and highly desirable that no spatial scanning capability be included in the polarimeter design. These factors are particularly important to keep the instrumental polarization to a minimum. With care the instrumental polarization of a carefully designed polarimeter can be kept to less than 0.5%.

The potential adverse effect of sequential sampling of orthogonal polarization components , i.e., false polarization, has been discussed extensively above. Thus, the choice here is clear-cut unless a high frequency, stress-birefringent approach (or an equivalent method) is used. It is normally desirable that a polarimeter have the capability to determine the azimuth of the scene polarization, even though in many cases the azimuth can be established from the viewing geometry. In particular, for a spaceflight polarimeter it is even more desirable to have this capability, since it can provide an additional cross check of instrument calibration. A halfwave retarder positionable in azimuth provides a convenient way to determine the scene polarization azimuth (requires two retarder orientations with a two-beam polarimeter). In addition, a third retarder orientation rotated by 45° to one of the other two positions provides a simple means to cross-calibrate equivalent detectors by interchanging their polarization sensing roles.

Table 2-1. Tradeoffs Among Polarimetric Measurement Methods.

System Characteristic	Polarimetric Accuracy — High[1] ⟵ ⟶ Low[2]		
Telescope/Fore Optics Design	Symmetrical/Small Incident Angles/No. of Mirrors Small	- - - - - - -	Asymmetrical/Large Incident Angles/No. of Mirrors Large
Instrument Spatial Scanning	None	- - - - - - - - - - -	Many Mirrors/Large or Variable Incident Angles
Polarization Component Sampling	Simultaneous Pol. Component Sampling	- - - - -	Sequential Pol. Component Sampling
Azimuth Determination	⟵ Orientation of Halfwave Retarder Fast Axis[3] →⟵	Orientation of Principal Direction of Single Beam Analyzer[3] →⟵	None[4]
Signal-to-Noise Ratio (SNR)	SNR > 1000	- - - - - - - - - - - - - -	SNR < 100

Notes:

1. With high polarization accuracy the linear polarizance is determined to within better than 0.2% for low polarization (near 10% or less) and to within better than 1.0% for high polarizations (near 100%).

2. With low polarimetric accuracy the linear polarization is determined to within 1% or worse for low polarizations and to within a few percent or worse for high polarizations.

3. Effect on accuracy is dependent on exact implementation selected for retarder or single beam, e.g., dichroic, polarizer.

4. Without a determination of the azimuth of the scene polarization, the polarimetric error can be very large unless the scene polarization azimuth nearly coincides with one of the two (orthogonal) measurement azimuths.

The signal-to-noise ratio (SNR) of the measurement system determines the precision of the polarimetric measurement. It is clear that the accuracy of the measurement cannot be better than the precision limits set by the SNR. (The precision and accuracy would be identical if there were no calibration error.) The detailed propagation of error due to the SNR is dependent on the particular measurement method selected. As a general rule, it should be assumed that an SNR of greater than 1000 is required for quantitative polarimetric analysis.

2.3 SYSTEM MATHEMATICAL CHARACTERIZATION

In this subsection a number of characteristics of the general approach selected as most suitable for spaceflight polarimetric measurement at the outer planets mission will be described in terms of the Stokes vector/Mueller matrix formalism. A convenient way to describe the characteristics of the scene spectral radiance is in terms of the Stokes vector, usually denoted by {I, Q, U, V}, where { } denotes a column vector (see for example, W. A. Shurcliff, *Polarized Light--Production and Use*, Chap. 2, Harvard Univ. Press, Cambridge, Mass. (1962)). These components can be expressed in terms of measurements of the scene spectral radiance as:

$$
\begin{aligned}
I &= L_{0°} + L_{90°} = L_{45°} + L_{135°} \\
Q &= L_{0°} - L_{90°} \\
U &= L_{45°} - L_{135°} \\
V &= L_{rcp} - L_{lcp},
\end{aligned}
$$

(1)

where $L_{x°}$ are spectral radiance values measured with an ideal linear polarizer at azimuths $x°$ relative to a selected reference direction, and L_{rcp} and L_{lcp} are similar measurements made with ideal right and left circular polarizers, respectively. As noted previously, for the scenes of interest the circular polarization is negligible, and, with V set equal to zero, it is convenient to express the Stokes vector in the form:

$$
\begin{bmatrix} I \\ Q \\ U \\ V \end{bmatrix} = \begin{bmatrix} L_{0°} + L_{90°} \\ L_{0°} - L_{90°} \\ L_{45°} - L_{135°} \\ 0 \end{bmatrix} = \begin{bmatrix} L_u + L_p \\ L_p \cos 2\alpha \\ L_p \sin 2\alpha \\ 0 \end{bmatrix}
$$

(2)

where L_u is the unpolarized portion of the scene spectral radiance, L_p is the linearly polarized fraction of the scene spectral radiance, and α is the azimuth of the linearly polarization component relative to the selected reference direction. In this case, the degree of linear polarization, $P = L_p/(L_u + L_p)$ and azimuth, α, are given by:

$$
P = \frac{\sqrt{Q^2 + U^2}}{I} \quad \text{and}
$$

$$
a = \frac{1}{2} \arctan (U/Q).
$$

(3)

While four different radiance measurements are shown in the expressions for the two equivalent data sets, i.e., the I, Q, U, the L_u, L_p, α, or the I, P, α data sets, only three of the

measurements are independent. For example, $L_{135°}$ can be eliminated from the I, Q, U data set, since

$$U = L_{45°} - L_{135°} = 2L_{45°} - I = 2L_{45°} - L_{0°} - L_{90°}. \tag{4}$$

The Mueller calculus is convenient to represent the modifications to the Stokes vector produced by transmission through one or more optical elements.(ibid., Chap. 8). In general, the 4 by 4 element transmittance Mueller matrix [M] relates the resultant output Stokes vector {I*, Q*, U*, V*} to the Stokes vector of the incident beam, i.e.,

$$\begin{bmatrix} I^* \\ Q^* \\ U^* \\ V^* \end{bmatrix} = [M] \begin{bmatrix} I \\ Q \\ U \\ V \end{bmatrix} \tag{5}$$

With an actual sensor system, the final form of the measured quantities usually are voltages or data numbers (DN) and it is convenient to represent an end-to-end polarization sensor channel by a system Mueller matrix [M_S] that has units of spectral radiance responsivity, e.g., DN per unit of spectral radiance. In this case, the vector {S_0, S_1, S_2, S_3} representing the system output is given by

$$\begin{bmatrix} S_0 \\ S_1 \\ S_2 \\ S_3 \end{bmatrix} = [M_S] \begin{bmatrix} I \\ Q \\ U \\ V \end{bmatrix} = [M_S] \begin{bmatrix} L_u + L_p \\ L_p\cos 2\alpha \\ L_p\sin 2\alpha \\ 0 \end{bmatrix} \tag{6}$$

where the assumption of no circular polarization in the scene is explicitly included in the Stokes vector of the scene. For an perfect polarimeter consisting of an ideal positionable halfwave retarder followed by an ideal polarizing beamsplitter, the system matrix M_S has the form

$$[M_S] = R_x T_x [P(\phi)] [R(\pi,\rho)] \tag{7}$$

where R_x and T_x are the system responsivity and system optical transmittance, respectively, for channel "x", e.g., 0° or 90°; [P(ϕ)] is the Mueller matrix for an ideal linear polarizer oriented with transmission axis at azimuth ϕ to the reference direction (0°); and [R(π,ρ)] is the Mueller

matrix for an ideal halfwave retarder, i.e., with retardance $\Delta = \pi$. Upon matrix multiplication this becomes

$$[M_S] = \frac{R_x T_x}{2} \begin{bmatrix} 1 & \pm(\cos^2 2\rho - \sin^2 2\rho) & \pm 2\cos 2\rho \sin 2\rho & 0 \\ \pm 1 & \cos^2 2\rho - \sin^2 2\rho & 2\cos 2\rho \sin 2\rho & 0 \\ 0 & 0 & 0 & 0 \\ 0 & 0 & 0 & 0 \end{bmatrix} \quad (8)$$

where ρ is the orientation of the fast axis and the upper sign corresponds to the 0° polarization channel and the lower sign the 90° channel.

For an actual instrument there will be departures of the components from the ideal, and for the selected polarimeter approach the major departures can be expected to be in the halfwave retarder. This is due to the difficulty of achieving near perfect achromatism of the halfwave retarder over the desired spectral range. As discussed in Section 3, the superachromatic halfwave retarder design will show small departures in both retardance and fast axis orientation versus wavelength. In contrast, a Wollaston prism is a near ideal polarizing beamsplitter with an extinction ratio typically exceeding 10^5. Thus, the Mueller matrix representation for each channel of the two-beam polarimeter can be represented to good approximation by

$$[M_S] = \frac{R_x T_x}{2} \begin{bmatrix} 1 & \pm[C^2 - S^2 \cos \delta] & \pm[SC(1 + \cos \delta)] & \pm S \sin \delta \\ \pm 1 & C^2 - S^2 \cos \delta & SC(1 + \cos \delta) & S \sin \delta \\ 0 & 0 & 0 & 0 \\ 0 & 0 & 0 & 0 \end{bmatrix} \quad (9)$$

where $C = \cos 2\rho'$ and $S = \sin 2\rho'$ where $\rho' = \rho + \varepsilon$ is the actual fast axis orientation and ε indicates the departure from the nominal direction (at some reference wavelength); δ is the departure of the retarder from the ideal, i.e., $\Delta = \pi + \delta$; and the sign convention is as in Equation 8. Thus, the measured signals, i.e., corresponding to the S_0 term of Equation 6, are given by

$$S_{0,x}(\phi) = \frac{R_x T_x}{2} \left\{ I \pm Q(C^2 - S^2 \cos \delta) \pm USC(1 + \cos \delta) \right\} \quad (10)$$

when $V = 0$.

The instrumental constants representing the assumed instrumental error conditions are the retardance error δ and the fast axis orientation variation ε. In addition, the effective responsivity

ratio $(R_0 T_0)/(R_{90} T_{90})$ is require to calibrate the polarimeter. A convenient set of measurements for these determinations are with $2\rho' = 0°$, 45° and 90°. The responsivity ratio can be determined by viewing an unpolarized source as the product of the 0°and 90° channel signal ratios for the $2\rho'$ = 0° and 90° measurements. Any instrumental polarization can be determined during the same sequence of measurements by also taking a second set of data with the instrument rotated by 90° about the viewing direction. Comparison of the measured degree and azimuth of the polarization allows separation of any residual source polarization from the instrumental polarization. This can be done since the azimuth of the instrumental polarization will follow any instrument rotation, while the azimuth of any source polarization will remain fixed relative to the source. Both δ and ε can be determined using an input of linearly polarized flux into the polarimeter. Evaluation of δ requires measurements with the flux polarized at two different azimuths. The value of ε is the difference between the known polarization azimuth of the input flux and the measured (calculated) polarization azimuth.

As previously noted, only three appropriately selected measurements are required for scene linear polarization and azimuth determination. Thus, two retarder orientations are sufficient with a two-beam polarimeter. A single retarder orientation is sufficient where the positioning can be selected to align the effective sampling directions with the scene polarization azimuth. To take advantage of scene viewing situations where this is practical, such a capability has been made a part of the recommended approach.

2.4 FALSE POLARIZATION

An important distinction between the two basic types of polarimeters arises whenever a change in the observed scene radiance occurs between measurements at different analyzer orientations. Such a scene radiance variation causes a "false polarization" for a single-beam polarimeter, but results in little or no error with a two-detector, birefringent polarimeter. In this case, calculation of the polarization from these measurements will yield the magnitude of the false polarization directly. To indicate the effect on polarimetric accuracy due to false polarization resulting from various classes of polarimeters, three examples are described below.

The determination of the Stokes parameters I, Q, and U using a single-beam polarimeter is accomplished by measuring the intensity, $I(\phi)$, passed by an analyzer at three orientations

specified by the angle ϕ between the analyzer transmission axis and the reference direction. For a perfect instrument the intensity is given by:

$$I(\phi) = 1/2 \, [I + Q \cos 2\phi + U \sin 2\phi]. \tag{11}$$

Assuming that measurements are taken at 0°, 60°, and 120° and that the varying scene radiance results from uniform changes ΔI, ΔQ, and ΔU in the Stokes parameters between observations at successive analyzer positions, the false polarization arising from the change in the scene radiance is:

$$\begin{aligned}
\Delta P_m = \;& (- \cos 2\alpha - 1/\sqrt{3} \sin 2\alpha - P_m)\Delta I/I_m \\
& + (1/2 \cos 2\alpha - 1/\sqrt{3} \sin 2\alpha + 1/2 \, P_m) \, \Delta Q/I_m \\
& + (\sqrt{3}/6 \cos 2\alpha - 3/2 \sin 2\alpha + \sqrt{3}/6 \, P_m) \, \Delta U/I_m, \tag{12}
\end{aligned}$$

where the subscript denotes measured values and α is the azimuth of the linear polarization. Intensity changes, $\Delta I/I$, for a scanned scene are typically at least an order of magnitude larger than the corresponding values for $\Delta Q/I_m$ and $\Delta U/I_m$, e.g., if $\Delta I/I_m$ were 10%, then $\Delta Q/I_m$ and $\Delta U/I_m$ typically would be less than 1%. Thus, the magnitude of the false polarization is essentially the product of $\Delta I/I_m$ and a term on the order of unity. This would produce unacceptable errors for many observing scenarios.

A two-beam polarimeter—which has equivalent detectors in each beam—requires the equivalent of at least two orientations to obtain the first three Stokes parameters assuming the azimuth is unknown. A halfwave retarder located on the scene side of the Wollaston prism and positioned at two different azimuths can provide—in a simple manner—the optical equivalent of a rotation of the Wollaston prism. When a halfwave retarder is used, the intensities for the principal directions of the Wollaston, i.e., 0° and 90°, as measured by a perfect instrument are given by:

$$\begin{aligned}
I_0(\rho) &= 1/2 \, [I + Q \cos 4\rho + U \sin 4\rho], \text{ and} \\
I_{90}(\rho) &= 1/2 \, [I - Q \cos 4\rho - U \sin 4\rho], \tag{13}
\end{aligned}$$

where ρ is the angle between the retarder fast axis and the 0° direction. With assumed Stokes parameter changes ΔI, ΔQ, and ΔU between successive halfwave retarder measurements from $\rho = 0°$ to 22.5°, the false polarization introduced for the two-beam polarimeter is given by:

$$\Delta P_m = (P_m \sin^2 2\alpha) \, \Delta U/U_m. \tag{14}$$

Thus, the false polarization caused by changes in the scene radiance would be negligible for low polarizations, i.e., on the order of 10% or less, where high polarimetric accuracy in most needed.

Section 3
APPLICATION TO CASSINI MISSION

Based on the science and instrumental considerations discussed in the previous sections together with Cassini mission constraints, an instrument concept for this mission was developed. This instrument is designated the Spectro-polarimeter Photometer (SPP), and the design has been tailored to the science objectives specific to the Cassini mission. As a result, certain key instrument feature tradeoffs have been made, and a three color, high-speed photometer has been added as an adjunct to the basic spectro-polarimetry instrumentation.

3.1 SPP INSTRUMENT SUMMARY

The SPP is a high-accuracy, multi-channel spectro-polarimeter and photometer designed to address key Cassini science objectives by acquiring a comprehensive database of polarimetric measurements of Saturn and Titan, and of Saturn's rings and icy satellites. The SPP spectro-polarimeter function provides simultaneous measurement of both orthogonal polarization components of the scene radiance for 32 near-contiguous spectral bands spanning the range from near ultraviolet (350 nm) to the near-infrared (950 nm). The SPP photometer function allows simultaneous measurements in three spectral bands for limb and ring stellar occultation measurements and for zodiacal light measurments during cruise. The approach is direct and does not require unusual spacecraft accommodations or untried technology to obtain the needed measurements. Key features of instrument design enable the SPP to maintain accurate inflight calibration and achieve the high accuracy polarimetry required to meet the science objectives. The science objectives, approach, key instrument features, and instrument parameters (Table 3-1) are given here, with detailed discussions covered in the later subsections.

Science Objectives:
- Retrieve vertical and horizontal distribution of cloud/haze properties in the atmospheres of Saturn and Titan including optical thickness, single scattering albedo, particle size, shape characteristics and refractive index
- Use the temporal variations in the degree and position angle of polarization to study changes in cloud/haze opacity, particle microstructure and composition
- Measure the polarimetric and photometric properties of Saturn's ring particles, and determine their impact on the latitudinal deposition of solar energy on Saturn
- Map the radial structure of Saturn's rings and obtain the ring opacity at visible wavelengths, including a measure of the dust distribution
- Map the polarimetric and photometric properties of Saturn's icy satellite surfaces to infer surface characteristics
- Map zodiacal light, look for nightside lightning on Saturn and Titan, and obtain stellar occultation observations

Table 3-1. Spectro-Polarimeter Photometer (SPP) Instrument Parameter Summary.

PARAMETER	INSTRUMENT CHARACTERISTICS
Telescope	Cassegrain-type (Dall-Kirkham), 15-cm Aperture Diameter, 75-cm Effective Focal Length (Galileo PPR Design Scaled up by × 1.5)
Memory Storage	64K × 16 RAM with 56K × 16 Allocated for Data Buffer, Additional Data Buffering in BIU (3 Blocks of 8.8K bits); 8K × 16 ROM Allocated for Instrument Operation Program
Commands/Modes	Six Mode Commands: Memory Keep-Alive and Verification (MKAV); Power-On Reset (POR); Spectro-polarimetry Azimuth Fixed (SPAF); Spectro-polarimetry Automatic Azimuth (SPAA); Spectro-polarimetry Azimuth Determined (SPAD), and Photometry Sampling Mode (PSAM); each Command Mode, except MKAV and POR, has Selectable Parameters Affecting Detailed Operation of the Modes
Electrical Interfaces	Signal to BIU via Manchester II MIL STD 1553B Serial Interface; Power via Balanced ± 15Vdc (Transformer Isolated at Instrument with Chassis Unipoint Ground)
Power	Typical Average Power = 4.8 W (Maximum Average Power = 5.5 W for Most Active Configuration); Peak Power = 9.2 W (80 msec Pulses). [Note: BIU Peak Power not Coincident with Actuator Peak Power Pulses since either the CDS will read out the SPP only on Specific RTIs (Preferred Approach) or the SPP will be designed to sense the Lack of BIU Readout following Receipt of an RTI and only for the Remainder of Those RTI Periods will Retarder Actuator be allowed to Step]
Mass/Size	Mass = 6.8 kg; Size = 63 × 21 × 23.5 cm (Length × Width × Height)
Viewing and Pointing Requirements	Optical Axis Aligned Parallel to Other HPSP Instruments within 2 mrad (0.5 mrad Knowledge); Science Photometric Calibration Targets to be Viewable Occasionally; 5° Field of View (Full Angle) to be Clear of Obstructions; Direct Viewing of Sun to be avoided Except on Transient Basis
Temperature Limits and Thermal Control	Operating Range +40 to -40°C; (Preferred Operating Range 0 to -40°C); Non-operating (Survival) Range 50 to -50°C; SPP to be Conductively Isolated from HPSP with Thermal Control provided by Thermal Blankets/Surface Coatings and When Instrument Power off by Replacement Heater Power

	SPECTRO-POLARIMETRY	PHOTOMETRY
Spectral Bands	32 Bands (Δλ = 10 nm); Near-Contiguous Coverage 350-950 nm	Three Spectral Bands: 350-540 nm; 560-700 nm; and 720-950 nm
Instantaneous Field of View	0.5 mrad Square	8 mrad Circular
Spectral Separation Method	Out-of-Plane Czerny-Turner Grating Spectrometer Configuration with 300 lines/mm Diffraction Grating (λ_B = 500 nm) used in First Order	Two Dichroic Beamsplitters plus Three Bandpass Filters provide Spectral Separation for Simultaneous Detection in Three Spectral Bands
Detectors	Two 32-element, Multiplexed Linear Arrays with UV-Enhanced Silicon Response	Three UV-Enhanced PIN Silicon Photodiodes Identical to those used on Galileo PPR
Radiometric Calibration	Science Calibration Target; Inflight Calibration Lamp; Preflight Calibration based on Irradiance Standard Lamp (NIST referenced) used with Halon Reference Standard	Inflight Calibration based on Viewing Stars of Known Characteristics; Preflight Calibration based on Irradiance Standard Lamp (NIST referenced) used with Reflectance Standard plus Attenuation
Polarization Analyzer and Calibration	2-Element Wollaston Prism Analyzer; and Super-Achromatic Half-Wave Retarder (HWR); HWR Rotations by 22.5° and 45° provide 45° and 90° Scene Polarization Azimuth Rotations; HWR Positioning Capability in 3.75° Steps allows Fixed Azimuth Polarization Measurements	Not Applicable except for Pre-flight Characterization of Polarization Sensitivity
Analog-to-Digital Conversion	Simultaneous 14-bit A/D Conversion of Signals from the Two Detector Arrays; Spectral Normalization during Data Processing produces 12-bit Data Samples	Simultaneous 14-bit A/D Conversion of Signal Data from the Three Photometer Detectors; Block Renormalization and Truncation to 10 bits Eliminates Non-significant Data Sample Bits
Telemetry Rates	1024 bps provides Complete Retrieval for Highest Data Rate Modes; 256 bps allows All Spectral Bands with Temporal Aggregation or 10 bands without Aggregation; 64 bps provides Useful Rate with Aggregation and/or On-board Polarization Calculations; 8 bps for MKAV Mode	1024 bps for PSAM Mode provides > 4-minute Measurement Window (SPP Memory Buffers the 3 Kbps Internal Burst Data Rate); 256 bps for PSAM Mode allows > 3-minute Measurement Window; 64 bps Useful with Rate Reducing Data Processing and/or Temporal Aggregation; with Zodiacal Light Measurements or MKAV Mode
Measurement Accuracies	Polarimetric: ± 0.2% (Goal: ± 0.1%) Absolute Radiometric: ± 3% (Precision better than 1%)	Precision during Limb/Ring Measurements better than 0.5% for +1 mag Star at 100 sample/sec (Reference obtained by Viewing Star Before or After Occultation); Zodiacal Light Accuracy ± 10%; Star-based Accuracy ± 3%

Approach:
- Simultaneous measurement of radiance and linear polarization in 32 near-contiguous spectral channels from 350 to 950 nm
- Combined use of phase angle and multispectral radiance with degree of linear polarization to determine cloud/haze properties
- Simultaneous high speed photometric measurement in three channels (350-540, 560-700, and 720-950 nm) to map zodiacal light, look for nightside lightning and infer haze distribution and upper stratospheric temperatures from stellar occultation observations

Key Features:
- Simultaneous detection of orthogonal linear polarization components of scene radiance
- Routine capability to interchange (cross-calibrate) roles of detector elements used to detect orthogonal polarization components. Simultaneous spectral measurement of scene radiances and linear polarization degree in all SPP spectral bands
- Single instantaneous field of view (IFOV) to assure precise spatial registration of all polarimetric measurements
- Uniform detector responsivity across the full IFOV through the use of pupil imaging
- Inflight internal and stellar calibration sources to provide routine calibration for polarimetric and photometric measurements

3.2 CASSINI SPP EXPERIMENT SCIENTIFIC OBJECTIVES

The primary goal of the SPP experiment is to produce a comprehensive database of high-accuracy, spectrally-resolved polarimetric measurements of Saturn, Titan, and Saturn's rings and icy satellites that can be used for detailed modeling studies. The primary scientific objectives of the SPP experiment are to:

1. Retrieve the vertical and horizontal distribution of cloud/haze properties including their optical thickness, single scattering albedo, size, shape characteristics, and refractive index

2. Use the temporal variations in the degree and position angle of polarization to study changes in cloud/haze opacity, particle microstructure and composition

3. Measure the polarimetric and photometric properties of Saturn's ring particles to determine their impact on the latitudinal deposition of solar energy on Saturn

4. Map the radial structure of Saturn's rings and obtain the ring opacity at visible wavelengths, including a measure of the dust distribution

5. Measure and map the polarimetric and photometric properties of Saturn's icy satellite surfaces to infer surface macro/micro- structure

6. Map zodiacal light, look for nightside lightning on Saturn and Titan, and obtain a measure of stratospheric temperature structure from stellar occultation observations

Additional objectives of the SPP experiment include making spectro-polarimetric measurements during asteroid flyby to help characterize the target asteroid surface properties. The SPP will also acquire Jupiter flyby observations that extend the spectral and temporal coverage of Jovian observations beyond those of the Galileo mission.

Earthbased polarimetric observations of Saturn are restricted to a narrow phase angle range of 0 to 6.4°. Though inadequate for constraining quantitative analyses, they do show latitudinal gradients both in the degree and position angle of polarization, including time variable changes in the polar regions of Saturn. Polarimetric measurements from the Saturn Pioneer and Voyager flyby missions lacked a truly diagnostic capability but confirmed the variability of the polarization. What is urgently needed is a comprehensive and accurate polarimetric survey of Saturn, Titan, and Saturn's rings and satellites in order to map the spatial and spectral variations of both the degree and direction of polarization over the full range of phase angle.

The SPP observations also will provide essential support for other Cassini experiments. For example, accurate temperature retrievals require detailed knowledge of cloud and haze properties and their vertical distributions. Microstructure information inferred from polarimetry will aid in the interpretation of mineral band mapping of satellite surfaces. Zodiacal light measurements during cruise will help place interplanetary dust measurements into a broader context. SPP stellar occultation measurements will provide a measure of stratospheric temperature structures complimentary to radio science, IR limb-scan, and UV occultation results and will help to bridge the "information gap" in the poorly sampled pressure regime between radio science and UV occultation measurements.

3.3 PRIMARY MISSION CONSTRAINTS

Primary mission constraints are similar to those experienced on predecessor missions to the outer planets, namely:

1. Mass limitations which typically result in serious science capability versus mass tradeoffs being made by the mission project with the result being tight constraints on instrument mass

2. Power limitations which favor instruments with low average power requirements and reasonable peak-to-average power ratios

3. Data rate and command capability limitations which favors instruments that either make low demands on these resources or have substantial operational flexibility, thereby minimizing mission impacts

4. Operational compatibility with companion science instruments (such as those co-located on the high precision scan platform (HPSP)) which allows more optimal scene viewing strategies

5. Cost limitations which mean that strategies that enhance science capability versus cost and that minimize instrument development risks are favored

Clearly the above mission constraints are not independent and tradeoffs among these are both necessary and appropriate. As an example, to minimize mass the SPP design utilizes beryllium as the prime structural material at the expense of some additional material, manufacturing and assembly costs.

3.4 SPP INSTRUMENTATION

In this section the rationale for the instrument design in terms of required key features is discussed which is followed by a brief overview of the instrument design, operating characteristics, and performance. Details of the optical, mechanical, and electronic designs are covered in the remaining subsections.

Key Polarimeter Features

Realization of the advantages of the impressive information content inherent in polarimetry is contingent on making measurements with sufficient accuracy. Key instrument features necessary to achieve scientifically useful polarimetric accuracy, viz., of approximately 0.1% for low scene polarizations, are discussed below.

1. *Adequate signal-to-noise-ratio (SNR).* If all systematic errors are eliminated, the polarimetric error ΔP, is a function both of the SNRs of the individual polarization component measurements and of the degree of polarization, P. The need for a high accuracy is greatest when P is small, since the ratio of polarization error to polarization, $\Delta P/P$, is of greater importance in most scientific applications of polarimetric data than is ΔP. In general, SNRs must exceed 1000 to yield useful polarimetry, with higher SNRs desirable at the very low polarizations.

2. *Simultaneous measurement of orthogonal polarization components.* Measurement of orthogonal polarization components should be made simultaneously, since if different portions of the scene are viewed sequentially for the two components (due to pointing changes), spatial scene radiance variations can be interpreted as polarization differences, with such errors being designated as first order false polarization.

3. *Cross-calibration of detector channel responsivity.* Relative responsivity calibration is required between detector channels to achieve accurate polarimetry. The SPP provides such inflight calibration by rotating the fast axis of the halfwave retarder (HWR) by 45° (scene polarization azimuth rotated by 90°) which effectively interchanges the polarization sensing roles of detector channels sensing the orthogonal polarization components.

4. *Definition of the IFOV prior to the polarimetric separation.* First order false polarization can result even with simultaneous measurement of orthogonal polarization if both polarization components do not represent exactly the same instantaneous field of view (IFOV), i.e., exact spatial registration is also required. This is the prime defect of most "imaging" polarimeter designs and has led to serious polarimetric accuracy errors even when equivalent pixels are "calibrated" by viewing a uniform radiance calibration target.

5. *Uniform detector responsivity across the IFOV.* One well-proven technique to minimize IFOV differences is the use of pupil imaging, whereby the entrance pupil rather than the field is imaged on the detector. However, detector improvements leading to very uniform spatial responsivities, particularly for silicon photodiode detectors, makes this somewhat less important than in the past.

6. *Simultaneous measurement of all spectral bands.* Sequentially collected spectral polarimetric data may represent spatially different portions of the scene and, as a consequence, represent different scene polarization inducing processes. While this is clearly not comparable to the false polarization problem where scene radiance differences are mapped erroneously into apparent polarization (false polarization), lack of spectral simultaneity can impair the usefulness of the measurements. For this reason, the

instrument enhancement of providing simultaneous measurement at all instrument wavelengths has been included in the SPP design.

7. *Spectral coverage from the near-ultraviolet through near-infrared.* The choice of desired spectral coverage of the SPP has been described in some detail in the science approach section. The selected span from 350 to 950 nm satisfies the science goals with an instrument which impacts the spacecraft and project resources modestly with high scientific return. The need for the near-continuous spectral coverage is important when the spectral dependence of the scene is poorly known.

Effect of Key Polarimeter Features on Selection of SPP Design

The above requirements taken together significantly limit the instrument configurations that are capable of performing the required polarimetric measurements. Among the key features listed, the first four are considered "essential" for serious polarimetry and form the basis for eliminating most alternative polarimeter designs. Alternative approaches were studied with an initial goal of achieving increased spatial coverage and/or simultaneous spectral coverage. The resultant SPP polarimetry approach selected is based on a positionable superachromatic halfwave retarder and a Wollaston prism providing the polarization component selection and separation with this combination being integrated within a grating spectrometer. Two linear arrays located in the exit plane provide the simultaneous sensing of the orthogonal polarization components in 32 spectral bands. To provide insight into the basis for this selection, the characteristics of major alternative approaches vis-á-vis the key polarimeter features are summarized below.

Area array(s) with simultaneous sensing of orthogonal components and sequential wavelength measurements. Regardless of the approach selected for performing the polarimetric separation/sensing, the use of two area arrays to sense "images" in two orthogonal polarizations poses insurmountable alignment/registration/pixel responsivity variation problems for achieving accurate polarimetry unless each individual IFOV is defined prior to polarization separation (Condition 4 above). A further disadvantage of such an "imaging polarimeter" approach is the lack of spectral simultaneity of measurements. While the lack of spectral simultaneity of measurements rates lower in importance than polarimetric accuracy, spectral simultaneity is a distinct asset whenever scene line-of-sight changes are relatively rapid.

Area array(s) with both simultaneous polarization component and wavelength sensing. Another area array approach that was investigated was the use of an area array in the exit plane of a spectrometer, where one dimension of the array provided spatial coverage and the other dimension spectral coverage. This approach does not satisfy condition 4 above, unless the entrance IFOV array is defined with separate IFOVs which would allow the effects of non-ideal imaging between the entrance and exit planes to be accommodated by using over-sized detectors in the spatial direction (typically the imaging is astigmatic with the choice made to have the greater blur in the non-dispersive direction). However, achieving this condition, e.g., with the

use of a staggered bi-linear array of IFOVs in the entrance plane, would reduce substantially the number of spectral elements that can be accessed. Accordingly, this approach was deemed less desirable than the simpler approach selected for the SPP using two linear arrays located in the exit plane of a grating spectrometer for sensing orthogonal polarization components of the scene.

Single area arrays approaches. Modifications to imagers to convert them to "imaging polarimeters" typically take the form of positioning a polarizer in the optical path with sequential measurement of the polarization components. This approach will suffer from false polarization since registration to a small fraction of a pixel for sequential polarization component measurements is unreasonable to expect during typical scene viewing. Furthermore, such an approach does not offer the desirable feature of simultaneous spectral measurements.

Polarimeter modification to a wedge filter spectrometer. A modification of the Wedge Filter Spectrometer to permit simultaneous measurement of orthogonal polarization components has the defect that the spatial information content is mapped into the spectral domain which means that spatial scanning is required to produce complete spectral information for a given spatial element. Since this requirement would impose unreasonable constraints on HPSP control, this makes it an unacceptable choice for a mission such as Cassini.

Alternative approaches based on predecessor polarimeters. An alternative approach using two single detectors in conjunction with a filter wheel, such as has been used on Pioneer Venus Orbiter Cloud Photopolarimeter (CPP) and the Galileo Photopolarimeter/Radiometer (PPR) instruments, is viable for Cassini requirements. The basic approach used on these instruments provides two-beam polarimetry with a single IFOV defined prior to polarization separation, polarization separation by a Wollaston prism, detector cross-calibration and azimuth determination provided via halfwave retarders, and entrance pupil imaging on the detectors. This approach as implemented in the CPP and PPR instruments has the demonstrated capability of providing polarimetric accuracy in the 0.1 to 0.2% range for low polarization scenes. The proposed SPP instrument offers these same capabilities together with near contiguous and simultaneous spectral coverage from 350 to 950 nm (rather than the sequential measurements in a few spectral bands with a filter wheel instrument).

Another alternative design approach is the use of dichroic filtering, e.g., such as that used on Pioneer 10 and 11 Imaging Photopolarimeter (IPP) instruments, to provide simultaneous spectral measurements. This multi-function instrument had limited spectral coverage due to the use of a photoemissive detectors to perform the diverse functions of spin-scan imaging and polarimetry at Jupiter (and later at Saturn) plus the zodiacal light measurements during interplanetary cruise. While dichroic filtering approaches with an appropriately designed polarimeter are

viable, the greater spectral flexibility and much greater number of accessible spectral bands of the selected SPP approach was the primary basis for eliminating this approach.

Single-beam polarimeters with a single IFOV using sequential measurement of orthogonal polarization components clearly are subject to false polarization whenever scene changes occur between component measurements, e.g., due to relative spacecraft-to-scene motions. Thus, Voyager PPS-type instruments are unsuitable for a Cassini type application where polarimetric accuracies of better than 0.5 percent are required.

Key SPP Photometer Features

For limb/ring stellar occultation measurements simultaneous spectral coverage in three spectral bands is important to achieve the stated SPP science objectives. Excellent linearity, near uniform response across the photometer IFOV, typical SNR values of a few hundred, and selectable sampling rates up to 100 samples per second are all important requirements. The IFOV needs to be sufficiently large to minimize pointing difficulties and to assure that the star remains within the field for useful measurement times, including during limb measurements when atmospheric refraction changes the apparent line-of-sight. Stray light response needs to be minimized to increase measurement possibilities. However, for this application high radiometric accuracy is not required since a reference measurement is obtained before and/or after each limb/ring measurement. Operational features needed to accomplish the photometry functions are given in the modes of operation subsection.

For zodiacal light measurements with the photometer the product of aperture and solid angle needs to be sufficiently large to obtain useful SNRs. Flexible sample aggregation and dynamic range optimization features are essential to permit a useful measurement program. A star-based radiometric calibration is appropriate for this application of the photometer.

Summary Description of Instrument Design Selected

The SPP instrument design provides the dual functions of both a high-precision spectro-polarimeter and a high-speed photometer to support the science objectives of the Cassini mission. The SPP spectro-polarimeter function provides simultaneous measurement of both orthogonal polarization components of the scene radiance for 32 near-contiguous spectral bands spanning the range from near ultraviolet (350 nm) to the near-infrared (950 nm). The SPP photometer function (which shares the same telescope and has a field of view adjacent to the polarimeter) provides simultaneous measurements in three spectral bands at sampling rates up to 100 samples per second to allow limb and ring stellar occultation measurements. The SPP photometer will also measure zodiacal light during the cruise portion of the mission.

An exploded view of an instrument design that satisfies the requirements imposed by the science goals is shown in Figure 3-1. The elements of the design rely heavily on predecessor polarimeters built by SBRC and flown on several planetary missions. The telescope design is a scaled up version of the PPR telescope. The separate portions of the SPP telescope field of view are used for the spectro-polarimetry and photometry functions. This is achieved with a field stop that defines a 0.5 mrad square IFOV for polarimetry with the beam passing directly into the aft optics and an offset 8 mrad circular IFOV for photometry with the beam reflected into the photometry optics via the 45° fold mirror.
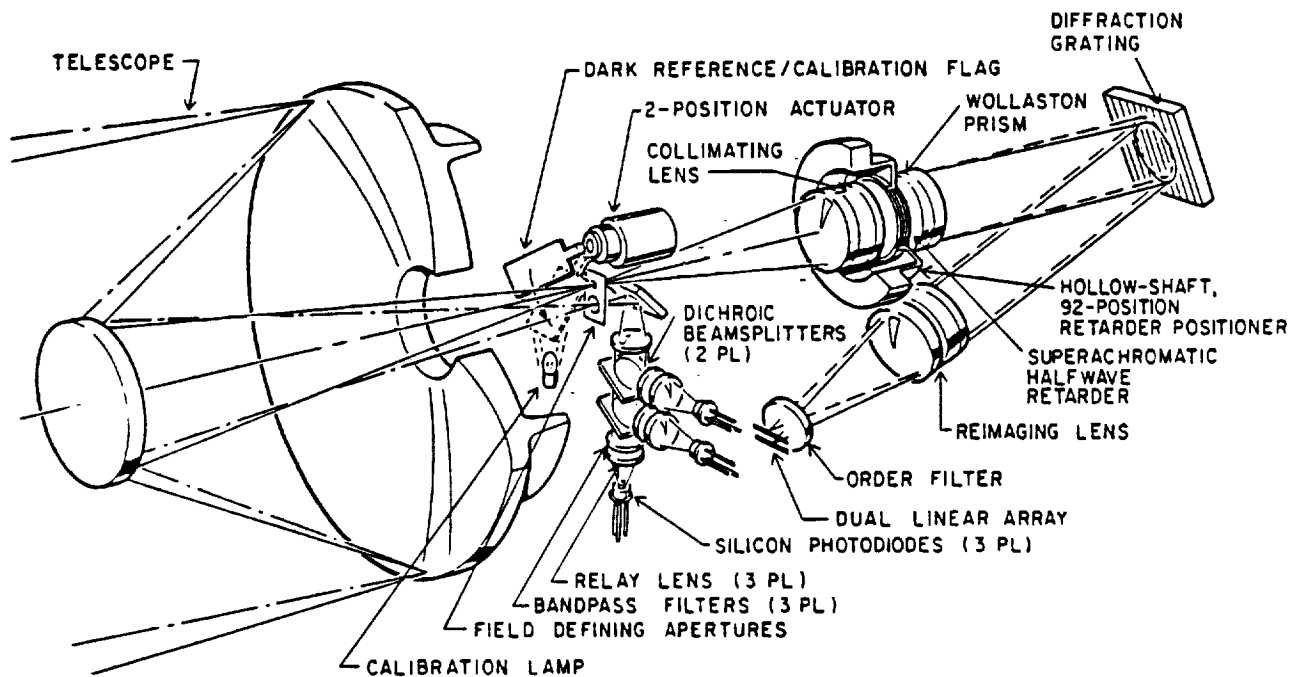
Figure 3-1. Exploded View of the SPP.

The polarimetry beam is collimated by a color corrected lens prior to passing through a halfwave retarder of near achromatic characteristics and then through a Wollaston prism. The Wollaston prism separates the orthogonal linear polarization components of the incident beam, thus resulting in two collimated, but angularly separated beams, incident on the diffraction grating. The spectrometer is an out-of-plane Czerny-Turner configuration with the two polarization components being spatially separated in the exit plane in the non-spectral direction. The 300 lines/mm grating blazed at 500 nm is used in first order and yields a near triangular spectral slit width of 10 nm across the SPP spectral range from 350 to 950 nm. The low blaze angle for the grating (4.3°) results in the grating efficiency being in the scalar regime, which gives optimum grating efficiency for the broad SPP spectral range. Furthermore, usage in the scalar region results in the grating efficiency being nearly the same for both polarizations.

(Detector channel responsivity cross-calibration eliminates the effect on polarization accuracy of differences of overall transmittance for the two polarizations.)

Following diffraction, the relay lens system refocuses the scene flux through the graded order filter and onto the two exit plane linear arrays. The location of the 32 elements of each array and the apertures of the associated exit plane aperture plate (which together with the field stop aperture determines the spectral content of the flux incident on each detector) are determined by ray tracing using the geometrical parameters of the spectrometer optical elements. To avoid introducing false polarization due to image quality and misalignments, the detector and aperture dimensions are made over-sized in the spatial (non-spectral) direction. The two 32-element linear arrays are multiplexed silicon photodiode arrays that offer a wide dynamic range and allow optimization of the spectral responsivity for the Cassini applications. Six selectable signal integration times and 14-bit analog-to-digital conversion of the preamplified array signals enhances the performance capability. Use of the nominal 1-second integration time provides adequate signal-to-noise ratios for most scenes of interest at Saturn without sample aggregation.

Figure 3-2 shows the SPP electronic block diagram and indicates the major functional elements of the electronics described in the Electronics subsection. The detailed operation of the SPP is controlled by macro commands uplinked to the SPP via the Cassini spacecraft command and data system (CDS). These macro commands select from among the various possible instrument operating routines and provide values for the selectable operating parameters. As discussed in the Electronics subsection, the SPP will interface with the project supplied Bus Interface Unit (BIU) for command and data transfer. The SPP microprocessor provides the detailed control of the detector readout, instrument mechanism operation, and signal processing/data editing. The primary instrument modes are listed in the operational modes subsection along with a brief description of the operational features.
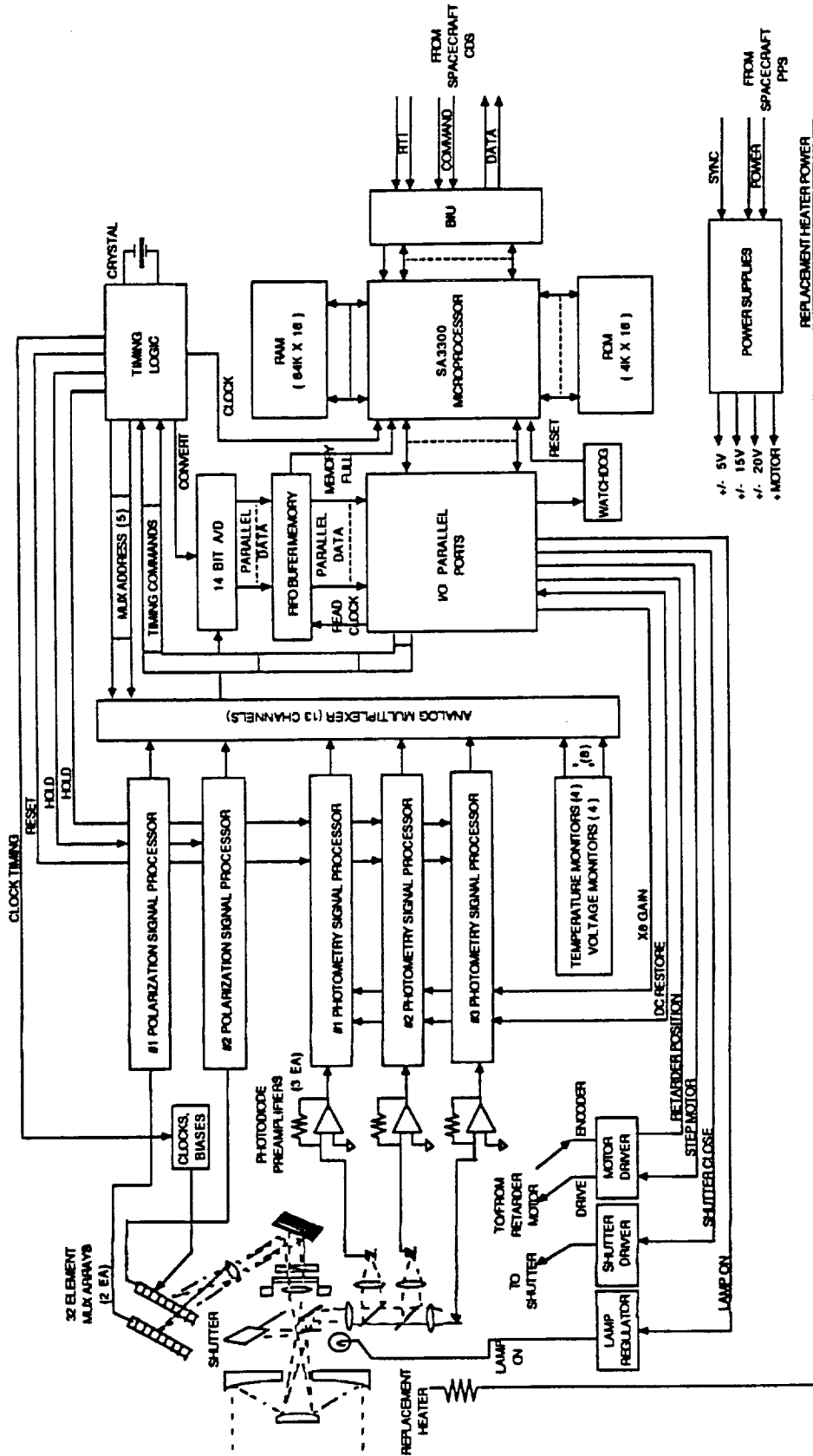
Figure 3-2. Spectto-Polarimeter Photometer (SPP) Electronics Block Diagram.

The key cross-calibration of the detector elements sensing orthogonal polarization components is achieved in the SPP by rotating the fast axis of the HWR by 45° which corresponds to twelve 3.75° steps of the retarder actuator. This provides the desired interchange of the roles of the S and P detector channels, since a 45° change of the fast axis azimuth produces a rotation of the azimuth of the incident linear polarization by 90°. Details of the achromatization of the HWR are discussed in the Optics subsection.

When measurements are taken with the HWR fast axis at two azimuths separated by 22.5°, the scene polarization (magnitude and azimuth) can be determined regardless of the polarization azimuth. While the SPP will have the capability of making polarization measurements in this manner, i.e., SPAD mode, an additional polarization measurement capability is included in the SPP design. This allows aligning the fast axis of the HWR to the scene polarization azimuth to within half a step of the retarder actuator. This fast axis alignment can be selected either by command, i.e., via SPAF mode when the plane of scattering is determined, or automatically using the SPAA mode. Since such polarization determinations using only the S- and P- measurements at one azimuth will produce an error of $P\sin^2\Delta\varepsilon$ (due to a misalignment $\Delta\varepsilon$ between the sampling and polarization azimuths). The maximum error from this source is 0.004P, i.e., 0.4% of the actual polarization. Such an error is quite acceptable since it gives a maximum polarization error of only 0.04% for polarizations less than 10%, i.e., significantly less than the SPP polarimetric accuracy of approximately 0.1%.

The dark reference/cal flag serves several functions when positioned in the optical path by means of the 2-position actuator. The prime function is to provide a dark background which yields the dark reference signal levels for the array detectors and allows dc-restoration of the three photometer channels. By energizing the calibration lamp when the flag is positioned in the beam, flux is directed into the spectro-polarimeter optical system. The resultant signals provide a means to monitor responsivity changes with time. Additionally, the flag can be commanded into the beam for instrument safety in the event the SPP is expected to be pointed at the sun other then on a transient basis, i.e., with a scan rate less than approximately 10 mrad/s.

The photometer portion of the SPP senses scene flux within the relatively large 8 mrad IFOV of the photometer. The optics consists of: (1) a fold mirror which directs the scene flux into the photometer; (2) a combination of a collimating lens and three sets of relay and field lenses; and (3) a set of two dichroic beamsplitters plus three trimming filters that define the 350 to 540 nm, 560 to 700 nm, and 720 to 950 nm spectral bands. The lenses are arranged to image the entrance aperture onto the detector to minimize point-source nonlinearities while maintaining near constant response across the IFOV. Near-redundant stops located within the photometer serve to reduce stray light. Three UV-enhanced silicon photodiodes identical to those used on

PPR sense the focused flux. Sequencing of the dark reference/cal flag into the beam provides a dark reference for occasional dc-restoration of the signal channels, or a "safe state" when direct viewing of the sun is expected. In the three analog channels, the integrator gain is selectable in one of two states to allow improved dynamic range utilization, e.g., for zodiacal light measurements the ×8 gain increase will allow near square-root improvement with sample aggregation by limiting digitization noise. Simultaneous sampling of the three detector channels and analog-to-digital conversion with the 14-bit ADC used for polarimetry provides the raw data suitable for further on-board processing. This processing includes selectable data aggregation and processing as indicated in the operational modes subsection.

Optical Design

A preliminary optical design has been developed for the SPP that includes both the spectropolarimeter and the photometer portions of the instrument that satisfy the stringent requirements imposed by the need for accurate polarimetry over a wide spectral range together with a high speed photometer capability. An exploded view of the SPP optical design was shown earlier as Figure 3-1. This consists of Cassegrain collecting optics, a positionable achromatic halfwave retarder, a refractive collimating triplet, a Wollaston prism, a diffraction grating, a refractive reimaging triplet, and an order filter adjacent to the exit plane. One linear detector array is employed for each polarization with the length of the array in the direction of dispersion. Ray tracing has verified acceptable image quality over a 350 nm to 950 nm spectral range for the preliminary design. While further improvement is expected with a detailed optimization, the detector array design can be sized and located to accommodate the present optical characteristics in a reasonable manner, and thus implementation of this preliminary optical design would not compromise any science goals. Similarly, ray tracing of a conservative preliminary optical design that uses pupil imaging for the photometer has verified that portion of the design. A description of the optical design elements follows.

Primary Telescope. The Cassegrain form of collecting optics was chosen for four reasons: (1) it can be manufactured in a very compact form; (2) the optical system is light in weight; (3) it has well-proven heritage from many previous instruments; and (4) perhaps most importantly, the radial symmetry of the design produces very little instrumental polarization. The telescope shown is a scaled up version of the Galileo PPR telescope (diameter scaled by a factor of 1.5). This Cassegrain telescope design provides an image quality far in excess of the SPP requirements as it can be diffraction limited across the 0.5 mrad field. While the telescope optics can be manufactured of glass, beryllium, or aluminum, it is felt that the requirements of the Cassini mission will be best satisfied by beryllium optics and telescope structure similar to that of the Galileo PPR. The 150 mm aperture is selected based on reasonable scene flux collecting requirements,

and an f/5 converging beam is selected for convenience as a manageable optical system. As with PPR, vapor deposited aluminum over the nickel-plated beryllium mirrors will be used for the reflecting surfaces.

Relay Optics. The key relay optics are the collimating and reimaging lenses. A refractive collimating lens for the Czerny-Turner spectrometer design (spectrograph configuration) was chosen to provide accessible space for location of the Wollaston prism and the retarder in a collimated beam. The refractive triplet illustrated perhaps represents a somewhat overly conservative approach for the collimating optics as the field of view is so small. However, it is necessary to maintain good color correction so that the longitudinal chromatic aberration does not introduce a strongly curved image surface. It is anticipated that a doublet lens design can be developed when the design is optimized further. The reimaging optics have a more difficult challenge as these must operate over the angular spread of the grating dispersion. For this application the relay design illustrated is very adequate as it produces an image blur at the detector plane equivalent to less than 2 nm of spectral width. Crystalline materials are used in the relay optics, and based on previous experience these should be more radiation resistant than most of the optical glasses. The lens surfaces will all be coated with spectrally broadband AR-coatings to reduce reflections between surfaces.

Halfwave Retarder. As discussed previously, the function of the halfwave retarder is to rotate the azimuth of the linear polarization components. The scene is alternately observed with the retarder fast axis at 0° and then at 22.5° to allow complete determination of the scene polarization via the 0°/90° and 45°/135° component measurements. (The scene linear polarization azimuth is rotated by twice the physical fast axis rotation.) A second function is to provide cross-calibration of the detectors sensing orthogonal polarization in each of the spectral bands. The third function is to provide the means to align the scene polarization azimuth parallel (or perpendicular) to the plane of deviation of the Wollaston prism. With the fast axis of the HWR adjusted to provide this condition, only the two simultaneously sensed orthogonal components are needed to compute the scene polarization. As discussed in the operational modes subsection, one SPP mode is an automatic inflight process to set the HWR fast axis so that the scene polarization azimuth lies within 3.75° of the Wollaston deviation plane, thereby allowing efficient, fixed-azimuth measurement sequences to be performed.

Since the halfwave retarder must function over the 350 to 950 nm spectral range covered by the SPP, it is necessary that the retardance be nearly achromatic over this spectral range. The required achromatization can be achieved by combining a Pancharatnam-type halfwave retarder (S. Pancharatnam, Proc Indian Acad. Sci. A41, 137, 1955) with an achromatic halfwave retarder (AHWR) constructed with achromatic combinations of two different birefringent materials

(D. Clarke, Optical Acta 14, 343, 1967; J. Beckers, Appl Opt. 10, 973 1971) to form a superachromatic design. (The former approach was used for the IPP HWR (S. F. Pellicori et al., Appl. Opt. 12, 1296, 1973), while the latter concept was applied in developing the CPP (S. F. Pellicori et al., SPIE 112, 28, 1977) and the PPR field widened HWRs using sapphire in combination with either MgF2 or crystal quartz depending on the spectral band.) Such superachromatic halfwave retarder designs have been described with calculated retardances within approximately 3° of the desired 180° from 280 to 1050 nm (K. Serkowski, p. 135 and J. Tinbergen, p. 175, in *Planets, Stars and Nebulae Studied with Photopolarimetry*, ed. T. Gehrels, 1974). This performance can be improved slightly for a similar design due to the reduced SPP spectral range.

While the combination of a positive ($n_e > n_o$) element with a negative element ($n_o > n_e$) provides a significant increase of angular aperture for the combination, a further degree of freedom is provided by the method suggested by Beckers (Appl. Opt. 11, 681, 1972). In this approach, one of the two elements is replaced with two elements of the same material (with the optical axes orthogonal) with individual thicknesses selected to provide both the required net thicknesses needed for spectral achromatization and the total thickness for maximizing angular aperture. One further factor of importance for SPP is the stability of retardance with temperature (see, for example, P. D. Hale and G. W. Day, Appl. Opt. 27, 5146, 1988), since it is planned that the SPP operate in the 0 to -40°C temperature range at Saturn to maximize detector performance. A detailed optimization and characterization of the superachromatic HWR design for the SPP application is desirable to minimize and simplify the calibration corrections to be applied to the measurements.

Wollaston Prism. A Wollaston prism has proven to be the best choice for separating an incident beam into two angularly-separated, orthogonally-polarized beams with the same beam characteristics and transmittance. Prisms of this type made with specially selected radiation re-sistant calcite have been used on all past SBRC polarimeters, i.e., Pioneer 10 and 11 IPP, Pioneer Venus Orbiter CPP, and the Galileo PPR instruments. The calcite material should be screened for radiation resistance in a similar manner to that used on the Pioneer and Galileo missions to Jupiter (S. Pellicori et al., Appl Opt. 14, 2618, 1979) to preclude the possibility of radiation darkening or fluorescence due to impurities in the calcite material. Due to the large differential expansion mismatch between the anisotropic prism elements, a construction technique developed for use on IPP (and subsequently used on the CPP and PPR instruments) is appropriate. This approach uses a high-purity, low outgassing silicone elastomer to bond the elements together and to bond them into an aluminum cell. Following this technique, three-element Wollaston prisms have been reliably temperature cycled over a -40°C to +50°C range. The two-element Wollaston

design for the SPP will be even less affected by temperature extremes. To reduce the effect of stray light from multiple reflections from the prism faces, it is appropriate to AR-coat the exterior surfaces with a broad-band AR coating.

From an optical viewpoint, the two polarizations need only to be physically separated at the image plane by an amount comfortably greater than the image blur. However, for ease of focal plane fabrication a nominal separation equivalent to five IFOV lengths has been selected corresponding to a physical separation of the two linear arrays of 1 mm in the exit plane. To provide this separation requires the interior angle of 3° for the calcite prism elements. This design can be altered easily to yield a greater or lesser deviation for the convenience of the focal plane design. The large birefringence of calcite makes it especially attractive for use in Wollaston prisms, since high birefringence permits adequate deviation with low aberrations. A ray trace approximation of a Wollaston prism which uses isotropic elements with refractive indices chosen equal to the ordinary and extraordinary refractive indices provides an excellent approximation for the small deviation and field angles of the present design. (At large deviation angles the isotropic material approximation yields a more pessimistic estimate of prism aberrations than an exact ray tracing of the crystalline components [M. C. Simon, Appl. Opt., 26, 3187, 1987].)

Diffraction Grating. As discussed previously, the spectrometer design selected (out-of-plane Czerny-Turner) has the grating oriented to provide out-of-plane dispersion. The selected grating has 300 lines/mm (grating spacing = 3.33 μm) with the blaze wavelength at 500 nm to approximately equalize the grating efficiency at 350 and 950 nm when the grating is used only in first order. A replicated grating is appropriate for this application as it has been found that replicated gratings usually provide higher grating efficiencies than original gratings and are less costly. (The particular grating selected is a standard catalog grating.) The very low blaze angle of this grating provides some significant advantages for the SPP application. These include the very nearly scalar theory behavior with the resultant broad range (between 2/3 and 1.8 times the blaze wavelength) where the grating efficiency exceeds 50% and the near equal spectral grating efficiencies for the two polarizations (E. Loewen et al., Appl. Opt. 16, 2711, 1977).

An out-of-plane angle of 15° is chosen for the SPP design to provide reasonable separation of the incident and diffracted light beams. The grating is rotated to provide a 5.4° angle of incidence to keep the 350 to 950 nm spectral range approximately centered, i.e., the diffracted angular range is spread equally about 5.4°. With a reimaging optics focal length of 60 mm, the 350 nm to 950 nm spectral range spans approximately 10.5 mm in the exit plane in the first order. Detailed ray tracing has been performed at three wavelengths, 390 nm, 650 nm, and 950 nm. In Figure 3-3 the image spot diagrams at the exit plane are superimposed on ideal images of the entrance aperture for the three wavelengths and two polarizations. It is seen that this

preliminary design has reasonable image quality. In terms of the ideal length of the image of the entrance aperture in the focal plane (pixel length), the worst case blur in the spectral direction for greater than 90% flux containment is approximately 0.2 of a pixel length (which is equivalent to 2 nm exit spectral width). In the spatial direction the worst case astigmatic image blur for 100% flux containment is about three times that length or 0.6 of a pixel length. At the center wavelength the astigmatism is negligible.

	390nm	650nm	950nm
a	0.2	0.1	0.2
	Image blur width for 90% of energy		
b	0.5	0.1	0.6
	Image blur height for 100% of energy		
c	2.9	2.5	2.7
	"Y" displacement of S polarization		
d	-2.4	-2.5	-2.0
	"Y" displacement of P polarization		
e	0.27	0.26	0.24
	Relative "X" displacement of P polarization		
f	1.6	1.6	1.6
	Detector size in "Y"		
g	1.0	1.0	1.0
	Ideal relayed IFOV length		
Dimensions are normalized to relayed IFOV length			
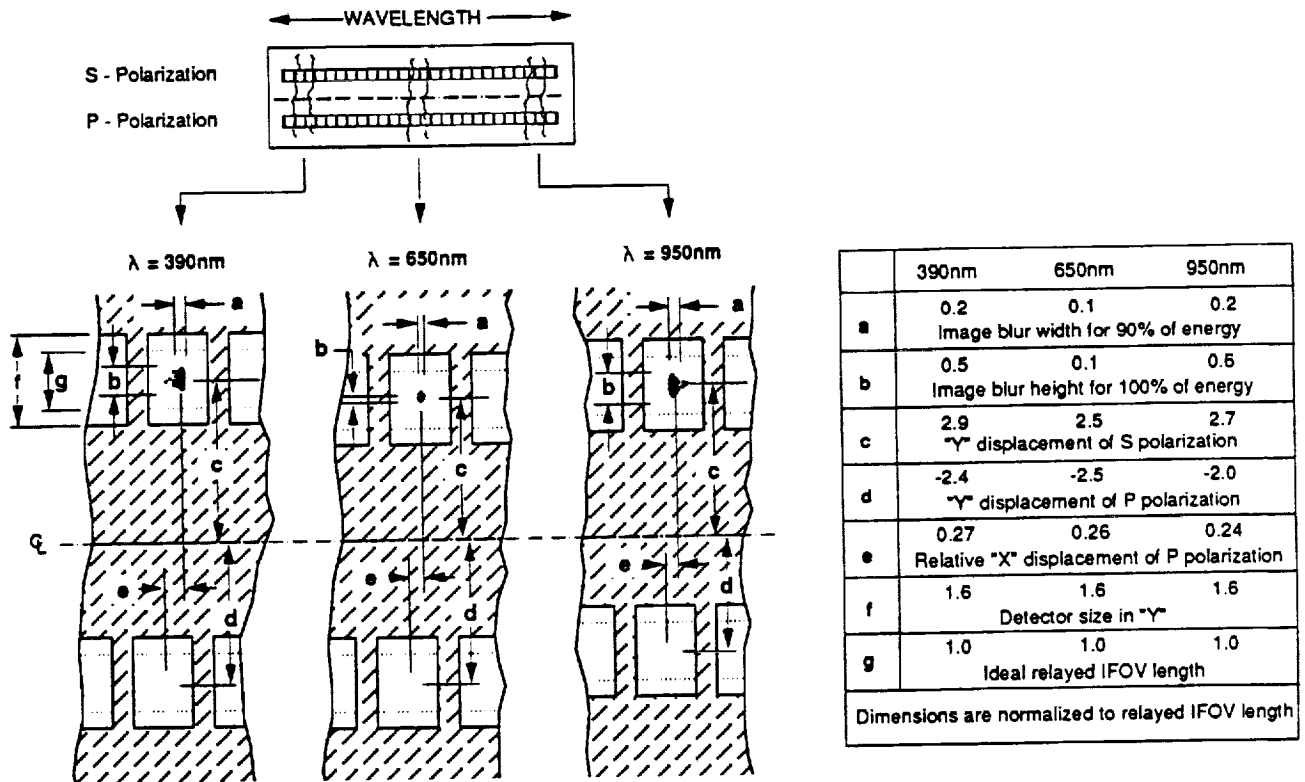
Figure 3-3. **Geometry of Detector Array with Image Blur for Preliminary SPP Optical Design.**

Focal Plane. The focal plane will consist of two closely spaced, linear arrays of silicon detectors. The detectors will be covered with an order filter to eliminate higher order diffracted light. It will not be possible to devise a suitable order filter with a single passband due to the wide spectral range. Two practical filtering approaches are: (1) the use of a set of three bandpass filters along the array length which are butted to each other; and (2) a filter with a linear variable bandpass (graded filter) along the array length. The latter approach is preferred, since it avoids the loss of spectral coverage in the butted regions.

With detector elements the same width across the array, the equivalent spectral width of the detectors would vary by about 2% across the array. Since such a small variation is not significant from the scientific viewpoint, the detector widths will be kept constant to simplify the array layout. Also, the detector length, i.e., the detector dimension in the spatial direction, will be made sufficiently oversize, e.g., 1.6 times the idealized image length or 0.30 mm, to assure that any image blur and misregistration does not cause false polarization.

Photometer Optical Design. The photometer is actually a separate instrument utilizing the same collecting optics. The telescope focal plane is shared with the photometer field offset from the polarimeter field stop. The flux from a star anywhere within the 8 mrad field of view of the photometer portion of the SPP is collected by the same telescope but diverted by means of a 45° fold mirror located behind the photometer field stop aperture. This mirror directs the flux towards the photometer optics shown in Figure 3-1. The combination of the collimating doublet and the three sets of reimaging and field lenses serve to focus the entrance pupil onto the 1.5 mm diameter active areas of the three silicon photodiode detectors. This pupil imaging approach is required, since imaging a sharply focused image of a star directly onto the detector would lead to intolerable errors caused by detector nonlinearity and/or detector spatial responsivity variations when a bright source fills an extremely small fraction of the field of view. Near redundant stops at the relayed aperture and field images are used to reduce out-of-field (stray light) response of the photometer.

The three broad spectral bands of the photometer are separated with two dichroic beam-splitters of conventional design, with spectral shaping provided by three spectral filters located in collimated beams of the photometer. This optical configuration allows simultaneous detection in all three photometer bands. As with the polarimeter optics, it may be possible to simplify this conservative design, e.g., remove one of the lenses from one or both of the doublets, during the detailed optimization of the design.

Instrument Performance

Instrument Signal-to-Noise Ratio. The signal-to-noise ratio (SNR) performance of representative individual array elements sensing the two polarizations are given in Table 3-2 for geometric albedos of 0.1, 0.3, and 1.0. The values presented are for single samples with a 1 second integration time and do not include noise associated with the determination of dark reference or gain calibration reference levels. The dark reference levels are established when the cal shutter blocks the scene with noise reduction accomplished during such measurements by aggregating samples. The primary responsivity calibration occurs when the SPP views the spacecraft Photometric Calibration Target (solar illuminated diffuse reflectance target) at one setting of the HWR

and another with the HWR rotated by 45° to provide the cross-calibration of equivalent array elements sensing the orthogonal polarization components.

Table 3-2.   Signal-to-Noise Ratio (SNR) Performance of Spectro-Polarimetery Function of the SPP at Saturn.

λ (nm)	$\Delta\lambda$ (nm)	T_0	K (note 1)	$H_\odot$ (w/[cm$_2$ nm])	$R_{det.rel}$	S_{scene} (e)	N_{shot} (e)	N_{dark} (e)	N_{reset} (e)	N_{amp} (e)	N_{quant} (e)	N_{total} (e)	SNR (p=0.3)	SNR (p=0.1)	SNR (p=1.0)
									{------ p=0.3 ------}						
350	10	0.122	0.982	1.12×10⁻⁴	0.36	5.03×10⁶	2242	1533	1327	35	1540	3392	1481	586	3475
400	10	0.176	0.982	1.65×10⁻⁴	0.45	1.83×10⁷	4282	1533	1327	35	1540	4982	3680	1722	7433.
450	10	0.208	0.982	2.15×10⁻⁴	0.58	3.51×10⁷	5926	1533	1327	35	1540	6449	5444	2744	10531
500	10	0.215	0.983	1.86×10⁻⁴	0.69	3.74×10⁷	6115	1533	1327	35	1540	6624	5645	2864	10885
550	10	0.210	0.984	1.87×10⁻⁴	0.82	4.37×10⁷	6608	1533	1327	35	1540	7081	6166	3173	11804
600	10	0.187	0.985	1.75×10⁻⁴	0.88	4.18×10⁷	6465	1533	1327	35	1540	6949	6016	3084	11539
650	10	0.175	0.987	1.61×10⁻⁴	0.95	3.89×10⁷	6236	1533	1327	35	1540	6735	5773	2939	11110
700	10	0.157	0.989	1.39×10⁻⁴	0.98	3.22×10⁷	5671	1533	1327	35	1540	6216	5173	2584	10054
750	10	0.140	0.991	1.27×10⁻⁴	1.00	2.76×10⁷	5256	1533	1327	35	1540	5840	4730	2324	9274
800	10	0.124	0.993	1.15×10⁻⁴	0.97	2.24×10⁷	4733	1533	1327	35	1540	5375	4168	1999	8289
850	10	0.115	0.995	1.00×10⁻⁴	0.91	1.70×10⁷	4127	1533	1327	35	1540	4849	3513	1628	7139
900	10	0.117	0.998	9.19×10⁻⁵	0.80	1.27×10⁷	3563	1533	1327	35	1540	4379	2898	1292	6057
950	10	0.120	1.000	8.35×10⁻⁵	0.55	7.34×10⁶	2710	1533	1327	35	1540	3719	1975	819	4399

Note: 1) K is transmittance factor resulting from selecting exit "slit" width such that exit spectral width is equal to entrance spectral width at 950 nm.

Parameters used: Telescope diameter = 15 cm with 20% obscuration; IFOV = 0.5 mrad square; f/number = f/5; $f_{collimating\ lens}$ = 12 cm; 300 ℓ/mm grating blazed for 500 nm used in 1st order in out-of-plane Czerny-Turner configuration with α = 5.4° and γ = 12°; $f_{relay\ lens}$ = 6 cm; two 32-element multiplexed silicon photodiode linear arrays in exit plane with Q_{sat} = 14 pC, I_{dark} ≤ 1 pA at 25°C corresponding to ≤ 0.38 pA at T_{oper} = 0°C (or below); T_{int} = 1 s; array readout time = 10 ms; C_{det} = 4 pF; $C_{video\ line}$ = 3 pF; C_{preamp} = 5 pF; preamplifier $\bar{e}_n$ = 10 nV/$\sqrt{Hz}$; and $QE_{det.pk}$ = 75% at 750 nm. Solar spectral irradiance at Earth $H_\odot$ taken from Neckel and Labs (*Sol. Phys.* 90, 205, 1984).

The SNR performance for the three spectral bands of the photometer portion of the SPP is given in Table 3-3 when viewing a +1 mag star of the same spectral type (G2V) as the sun. The performance is for single samples based on a sample rate of 100 samples/s. The key instrument parameters assumed are also included as part of the table. As discussed in the operating modes section, lower effective sampling rates can be produced by sampling aggregation with consequent improvement of SNR by the square root of the number of samples aggregated whenever the source viewed has a lower brightness. Also included in the table is the SNR performance when viewing the zodiacal light for brightness ranges equivalent to both 100 and 1000 S10 stars per square degree. For the zodiacal light scenes, sample aggregation times of 10 seconds (1024 samples) is assumed.

Table 3-3. Signal-to-Noise Ratio (SNR) Performance of Photometry Function of the SPP.

Type of Measurement (Note 1)	Scene Viewed (Note 1)	$\lambda_1-\lambda_2$ (nm)	$\Sigma H_0 T_0 R_d^2 \Delta\lambda$ (A/cm^2)	$f_{\Delta m}$ (Note 2)	S_{scene} (e)	N_{shot} (e)	N_{det} (e)	N_{preamp} (e)	N_{quant} (e)	N_{total} (e)	SNR (Note 3)
Limb/Ring	+ 1 Mag Star	350-540	4.89×10^{-3}	1.25×10^{11}	3.46×10^5	588	384	588	141	964	359
		560-700	4.56×10^{-3}	1.25×10^{11}	3.23×10^5	568	384	588	141	952	339
		720-950	4.94×10^{-3}	1.25×10^{11}	3.50×10^5	591	384	588	141	966	362
									(Note 3)		
Zodiacal Light	100 S10/deg^2	350-540	4.89×10^{-3}	4.97×10^{12}	1.44×10^3	38	384	588	18	752	61
		560-700	4.56×10^{-3}	4.97×10^{12}	1.34×10^3	37	384	588	18	751	57
		720-950	4.94×10^{-3}	4.97×10^{12}	1.45×10^3	38	384	588	18	752	62
	1000 S10/deg^2	350-540	4.89×10^{-3}	4.97×10^{11}	1.44×10^4	120	384	588	18	760	604
		560-700	4.56×10^{-3}	4.97×10^{11}	1.34×10^4	116	384	588	18	759	564
		720-950	4.94×10^{-3}	4.97×10^{11}	1.45×10^4	120	384	588	18	760	610

Notes:
1) Solar spectral distribution assumed for scene, i.e., G2V stellar spectral type.
2) $f_{\Delta m}$ = sun-to-star (or zodiacal light) magnitude difference expressed as a factor.
3) Limb and ring signal-to-noise ratios (SNRs) are based on single (10 msec) sample, while zodiacal light SNRs are based on aggregating 1024 samples plus increasing the amplifier gain by ×8 to reduce quantization noise.

Parameters used: Telescope diameter = 15 cm with 20% obscuration; IFOV = 8 mrad circular; A_{det} = 1.77×10^{-2} cm^2 (1.5 mm circular); R_{det} = 20,000 Mohm; T_{det} = 273K; R_{fb} = 10,000 Mohm; T_{fb} = 273K; T_{int} = 10 ms; T_{det} = 100 s; $\bar{I}_n$ = 0.6fA/$\sqrt{Hz}$; C_{in} = 55 pF (= C_{det} + C_{amp} + C_{stray}); $\bar{e}_n$ = 3.5nV/$\sqrt{Hz}$ with $f_{1/f}$ = 1 Hz; 14-bit quantization with full scale set to 8×10^6 electrons for ring/limb measurements and 1×10^6 electrons for zodiacal light measurements, i.e., integrator gain increased by ×8; solar spectral distribution assumed for stars based on irradiance values from Neckel and Labs (*Sol. Phys.* 90, 205, 1984).

Modes of Operation. The detailed operation of the SPP will be controlled by macro commands uplinked to the SPP via the Cassini spacecraft Command and Data interface. These macro commands will select among the various possible instrument operating routines and provide values for the selectable operating parameters as discussed in the Electronics subsection. The SPP microprocessor provides the detailed control of the detector readout, signal processing and data editing, and instrument mechanism operation. The primary instrument modes are listed in Table 3-4 along with a brief description of the operational features.

Table 3-4. Spectro-Polarimeter Photometer (SPP) Operational Modes.

1. **Memory Keep-Alive and Verification (MKAV) Mode.** This mode is the lowest power instrument "on" state and is intended only to service bus traffic, retain data and instructions that are resident in RAM, and provide a memory and housekeeping data readout at any allocated SPP readout rate.

2. **Power-On Reset (POR) Mode.** This is a preselected state that the SPP is initialized to when power is applied to the instrument. This mode will be the Spectro-Polarimetry Azimuth Fixed (SPAF) mode with the operating parameters set such that the mechanisms, i.e., the Cal Flag and HWR actuator are operated at a very low duty cycle. In POR 256 1-second samples are accumulated at a fixed HWR position followed by a sequence that includes dark reference samples (cal flag moved to block scene) and detector cross-calibration samples (HWR fast axis azimuth rotated by 45°.

3. **Spectro-Polarimetry Azimuth Fixed (SPAF) Mode.** This mode is a flexible version of the POR state in that the azimuth of the HWR fast axis is selected (via the HWR position command parameter) and data samples are accumulated for a selectable number of samples (1, 16, 64, or 256). Following this scene sampling, a selectable number of dark samples (0 [i.e., function disabled], 1, 4, or 16) are taken, a selectable cal lamp cycle with a selectable number of samples (0, 4, 8, or 16), and a selectable detector cross-calibration cycle with the numerical parameter (0, 1, 4, or 16) denoting the number of samples taken at each of the required HWR azimuth positions. The sample period is selectable from among 6 sample periods, i.e., 2, 3, 4, 6, 8, 12, or 16 RTIs (0.25, 0.375, 0.5, 0.75, 1.0, 1.25, 2.0 seconds, respectively) allowing optimization of the dynamic range.

4. **Spectro-Polarimetry Automatic Azimuth (SPAA) Mode.** This mode is similar to SPAF mode except that the fixed orientation of the fast axis azimuth of the HWR to be used for the measurement sequence is established by means of an automatic measurement sequence that determines the azimuth of the scene polarization. This is accomplished by cycling through five HWR azimuth positions (separated by 3.75°) and determining the azimuth where the polarization signals are extrema. For the remainder of the cycle this mode functions identically to the SPAF mode.

5. **Spectro-Polarimetry Azimuth Determined (SPAD) Mode.** In this mode the HWR is cycled through a selectable set of azimuths such as the 0°/90° and 45°/135° (or the 0°/90° and 45°/135° plus the 90°/0° when detector cross-calibration is included). From such measurements the scene polarization and azimuth can be determined regardless of the relation between the azimuth of the scene polarization and the HWR azimuth. Other measurement parameters can be selected as described for the SPAF mode.

6. **Photometer Sampling Mode (PSAM).** This mode activates and controls the various sampling/data processing options for the photometry channels. These include: selection of the level of sample aggregation, i.e., ×1, ×4, ×64, or ×1024; the readout method, i.e., continuous, time windowed, or event threshold windowed; and the detailed parameters of the readout method selected, e.g., such as the DN change from the running average which constitutes an event threshold.

Detector Selection

Three silicon detector configurations were considered for the two 32- element spectro-polarimetry arrays: (1) transparent gate charge coupled devices (CCDs); (2) discrete detectors with transimpedance amplifiers (TIAs); and (3) multiplexed photodiode detectors with off-focal plane amplification. Transparent gate CCDs which collect photo-charge under transparent polysilicon gates were eliminated because of their relatively low quantum efficiency and poor blue spectral response. The newer technology of thinning the silicon and illuminating the gates from the back side improves the overall quantum efficiency but not the blue response. Since the dynamic range of the CCD must be designed to prevent overload with the largest signal, smaller signals, such as those detected by the blue end of the array, have much reduced dynamic ranges.

Discrete detector arrays overcome the color balance problem because the detector anti-reflection coating can be optimized for the blue end of the spectrum. Also, the transimpedance preamplifier feedback resistance can be optimized for each detector, effectively matching the response of each element. Systems with as many as 96 element arrays are presently being manu-factured for the Enhanced Thematic Mapper instrument with the low-noise FET and feedback resistor for each detector mounted on a hybrid substrate along with the detector array. The

delicate assembly and high component count of analog processing circuitry would make this approach relatively costly for the 64 spectro-polarimeter channels.

The third alternative of multiplexed photodiode arrays offers a wide dynamic range and the advantage of anti-reflection coating optimization for color balance. It is also the least expensive because, unlike the discrete photodiode approach, it requires only a single electronic signal processing channel per detector array. These devices are fabricated using conventional P-N photodiodes connected to an output node with MOS transistor switches. An addressing network allows one detector at a time to be selected for read-out, and a "reset" switch connected to the output node applies a reverse bias to each detector after read-out. Signal current is integrated on the detector capacitance during the selected integration period, altering the bias charge placed on the detector at the previous "reset" time. At the end of the integration period, each detector output is sequentially read-out at a rapid rate (nominally 300 μs each). The output node signal is amplified by a low input capacitance preamplifier and subsequently digitized. While the multiplexed photodiode array approach has some disadvantages, overall it seems the best approach for the SPP application and is the "baselined" approach.

One disadvantage to multiplexed photodiodes is that exactly simultaneous sampling of each detector within an array is not possible, since they must be sequentially read out and reset. However, equivalent detectors in each array sensing orthogonal polarization components in a single spectral band can be read out simultaneously to assure this critical instrument feature. The integration time displacement can be minimized by more rapid readout at the expense of increased preamplifier noise bandwidth and consequently somewhat increased noise. It is reasonable that this displacement can be limited to 1% of the nominal 1-second integration time, i.e., that all array detectors be read out during a 10 ms period. This approach will not degrade the polarimetric accuracy since polarization pairs from each of the arrays are sampled exactly simultaneously.

Temperature control of the linear arrays to a temperature slightly above the surroundings is an appropriate means to achieve superior instrument stability. By providing levels spaced about 5° C apart throughout the SPP operating range, only a minor increase in instrument power would be required, i.e., less than 100 mW. This approach would improve array dark level (fixed pattern "noise") and responsivity stability, and thereby reduce the number of inflight and preflight calibrations required.

Incomplete charge readout is another factor that must be considered with the multiplexed photodiode approach. During the screening process for the flight arrays, a reasonable criterion for this parameter is that arrays that leave more the 0.5% (of the signal) residual charge are to be rejected for flight uses. However, even with less than 0.5% residual charge there may be in-

stances with rapidly changing scenes where this will cause unacceptable polarization error. To accommodate such conditions, the SPP can be commanded to operate the cal shutter to provide dark samples between every scene sample. Selection by command of this approach will assure quality scene data without the need to correct for effects from the preceding sample.

The detectors selected for the SPP photometer application are identical to those used in the PPR. These UV-enhanced, PIN silicon photodiodes have very high shunt resistances ($> 2 \times 10^9$ ohm at 25°C) for the 1.5 mm diameter active area. Since the thermal design of the SPP will maintain the optics operating temperature at 0°C or less, the detector resistance will exceed 2×10^{10} ohm during operation. The AR-coating which provides the UV enhancement also serves to increase the responsivity near the long wavelength cut-off and is optimal for the SPP application. Finally, while the radiation environment for the Cassini mission is less severe than for Galileo, the use of PPR-type detector housings is appropriate. These provide effective "spot" radiation shielding with minimal mass impact, thereby preventing loss of SNR performance due to either lowered responsivity or lower detector resistance with radiation dose.

Mechanical Design

The mechanical design of the Cassini Spectro-polarimeter Photometer (SPP) emphasizes the use of proven techniques and mechanisms to provide a high reliability instrument. The modular design selected allows testing of the individual assemblies prior to final assembly and facilitates the use of simplified final assembly techniques, while assuring that the required final optical alignments are achieved.

Mechanical Structure. A beryllium mainframe selected for high stiffness with low mass and excellent stability will house the following modular elements of the SPP: (1) telescope assembly; (2) the photometer assembly; (3) the spectro-polarimeter assembly; (4) the inflight calibration assembly; and (5) electronic module assemblies. The telescope is based on the PPR telescope flown on Galileo. The SPP telescope is slightly larger (15 cm versus 10 cm diameter) but retains the same proven design and mounting techniques. The primary mirror is beryllium and is mounted to the telescope structure via tangent bars to isolate the mirror from structural distortions. The photometer is an independent assembly that can be assembled, aligned, and tested prior to mating with the rest of the system. This assembly contains the folding mirror, two beamsplitters, shaping filters, relay optics, and three silicon photodiodes. The calibration assembly consists of a dark reference/calibration flag and associated actuator and a calibration lamp. The flag can be positioned to block the scene view and thereby provide either a dark reference or a known flux level when the calibration lamp is powered. This system is installed just forward of the optical image plane. The spectro-polarimeter assembly is contained in a separable module that includes the collimating lenses, Wollaston prism, diffraction grating, reimaging optics, order

filters, the dual linear arrays, as well as the halfwave retarder and associated positioning mechanisms. All of these optical-mechanical designs are based on concepts that have been proven in space on predecessor flight instruments or are being used on such instruments as TES and TIR currently being developed for the Mars Observer and CRAF missions, respectively. The material for the module frames is aluminum to provide radiation shielding in a relatively efficient manner. The design is totally modular, with each of the three modules containing either two single-sided or one double-sided printed wiring board. This results in a light weight design with excellent access to the electronics components. The much smaller photometer preamplifier and the linear array readout electronics boards are located in the optics housing.
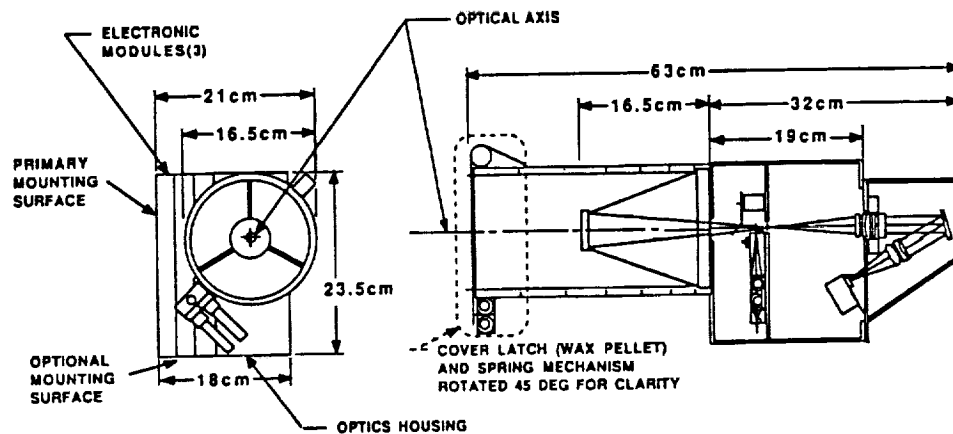

Figure 3-4. Cut-Away View of SPP.

The overall envelope of the SPP is 62 cm by 23.5 cm by 21 cm as shown in Figure 3-4. The mass of 6.8 kg is based, where possible, on the actual weight of past subassemblies. The mass estimate has also been cross checked against the densities of SBRC sensors of similar construction.

Table 3-5. Mass Breakdown for SPP.

Telescope/Cover and Actuator	1.60 kg
Structure	0.90 kg
Electronics Modules (including BIU)	2.60 kg
Photometer Assembly	0.23 kg
Spectro-Polarimeter Assembly	0.36 kg
Actuator, Halfwave Retarder	0.45 kg
Actuator, Dark Reference/Cal Flag	0.05 kg
Harnesses/Cables	0.55 kg
Miscellaneous Hardware	0.05 kg
Total	6.79 kg

Mechanisms. There are two mechanisms required for the SPP: the rotary actuator for the half-wave retarder; and the two-position actuator for the dark reference/calibration flag. Both mechanisms are relatively straight forward and will not require any "state of the art" designs. Similar mechanisms have been used by SBRC in a variety of sensor systems.

As discussed previously, the minimum requirement for the halfwave retarder actuator is that it provide rotation through a minimum of 45° in 3.75° steps (96 steps/revolution). However, a rotation capability through a full 360° is planned to allow full preflight polarimetric calibration characterization and to provide periodic 360° rotation to prevent lubricant "piling". Further requirements are that power be required only during retarder repositioning and that repeatability be better than 0.1°. To provide this function, a hollow-shaft, permanent-magnet stepper motor similar to those used on predecessor polarimeters is planned. The permanent magnet stepper ensures solid detent at each position even with power off, and a built-in encoder senses the position of the retarder element. Space qualified Braycote 601 grease is an appropriate lubricant for the bearings. Periodic rotation through several full rotations is planned to ensure full transfer of the lubricant to the balls and races. The estimated total mission life requirement of 2 million revolutions is well within the proven history of this mechanism.

The calibration shutter mechanism is a two-position, rotary actuator with a total travel of 30 degrees. An arm extending radially from the shaft of the actuator holds the dark reference/calibration flag, and a torsion spring holds the actuator out of the optical path in the normal operating (unpowered) position. A torque motor rotates the actuator into the optical path and allows the detectors to view either a dark reference or an illuminated surface depending on whether or not the calibration source is powered. The actuator is fail-safe in that if power is lost the spring returns the actuator to the normal operating position out of the field of view. The entire assembly is small, lightweight, and very little power is required to hold the shutter in the calibration position. The lubricant will be the same as for the halfwave retarder actuator, and the estimated mission life requirement of 16 million cycles is within the proven history of the device.

Thermal Control. The SPP can be designed to be thermally independent or coupled to the HPSP interface. Based on the allowable temperature range of the HPSP interface, it is tentatively planned to use thermal isolators at the mounting interface and thermal blankets and thermal finishes to control the radiation to space. This technique has been successfully used on previous sensors, and will allow the SPP to be operated colder than the HPSP, i.e., in the 0 to −40°C range, to improve the detector performance. With instrument power off for periods longer than approximately 2 hours, replacement heater power (approximately one half of the nominal SPP power) is required to assure an instrument temperature above −50°C.

Contamination Control. Standard contamination control practices such as assembly in a Class 100 flow benches, purging with dry nitrogen when possible, and storage in a sealed container when not in use is appropriate for minimizing particulate and molecular contamination of the SPP. During launch the optical system will be protected from dust contamination by a spring loaded aperture cover. When in space the cover will be released by actuation of a wax pellet actuator (Tibbits, Proc. 22nd Aerospace Mechanisms Symposium, p. 13 (1988)) and be held in the open position by the spring mechanism similar to that used on the PPR.

Electronics

Electronics for the SPP is designed to process the outputs of the three photometry detectors and two spectro-polarimeter arrays, control the shutter actuator and retarder motor positions as well as the inflight calibration lamp, provide the data processing/compression, and format the science and engineering data prior to transfer onto the spacecraft bus. The analog circuitry is similar to that of the PPR instrument, and the digital electronics and spacecraft interfaces are almost identical to the CRAF TIR instrument. The main differences from the predecessor instruments are in the array readout and data processing/compression which determine the telemetered SPP data packets. The functional electronics block diagram for the SPP was shown earlier as Figure 3-2.

Analog Signal Processing. Two identical polarimetry channels control and amplify signals from the two 32-element, multiplexed photodiode arrays, one array for each polarization component with the spectrum dispersed along the 32 element array length. These monolithic focal plane arrays have multiplexer scanning logic included within them, so only three clock drivers and a few bias voltages are required. Both arrays are clocked together so that the polarization pair samples are exactly synchronous. Photo-signals are integrated on the detector capacitance for any one of 6 selectable integration periods. During the array readout period of 10 ms following each integration period, the 32 outputs of each array are multiplexed onto the low capacitance node of the preamplifier. The preamplifiers are low input capacitance, voltage mode type with noise figures below those of the readout devices. Since all 32 detectors are readout in 10 ms, a preamplifier bandwidth of greater than 5 kHz is required to increase the signal level to a maximum of 10V and provide a low output impedance to drive the sample and hold capacitor.

Identical sample and hold circuits are used for all five analog channels. They are comprised of junction FET series switches which apply the analog signals to 5000 pF ceramic capacitors and are followed by FET input operational amplifiers. Series resistors are included in each signal path to limit the in-rush current and provide signal low-pass filtering.

The photometry channels each include a transimpedance preamplifier and DC-restoration circuitry as well as the gain stage and sample hold. Preamplifiers are comprised of FET input (low noise) operational amplifiers with feedback resistances of 1×10^{10} ohm. Signal bandwidths of greater than 300 Hz can be achieved with 1×10^{10} ohm resistors if the preamplifier first stage (and the feedback resistor) are hybridized with the detector. Detector capacitances of 50 pF can be tolerated before boosted preamplifier noise begins to affect the signal to noise performance. The electronics noise performance is dominated at all signal frequencies by feedback resistor thermal noise.

DC-restore circuitry removes the channel offsets caused by temperature drifts in the high gain preamplifier and the detector. The restore circuit operates like a sample and hold which samples the channel offset while the shutter is closed and subtracts the acquired "dark" value from subsequent data samples. (Hold times of 200 seconds have been used successfully for several SBRC space instruments operated in a range of environments.) DC-restoration occurs when the shutter is closed either under control of the instrument automatic modes or by ground command with both the dc-restore duration and the interval between dc-restores selectable by command. Data samples are telemetered both before and after restoration so that restore circuit performance can be constantly monitored and data can be corrected even if small drifts should occur. Signal low pass filtering is provided by a resetting integrator which is sampled then reset in the last 200 microseconds of each sample interval. A ground commandable x8 gain increase is included for zodiacal light measurements by switching a lower value input resistor into the integrator with a FET switch. Sample and hold circuitry is identical to that for the polarization channels.

The three photometry channels are simultaneously sampled (and digitized) every 10 milliseconds. The analog multiplexer is controlled by the timing logic and sequentially connects the analog "hold" values for each signal channel and the temperature and voltage monitor circuits to the 14-bit analog-to-digital converter (ADC). Several low power ADCs are available with 100 μs conversion rates. The maximum ADC output data rate is 300 14-bit words per second corresponding to the three photometry samples every 10 milliseconds.

The polarization channel amplifiers operate at a fixed gain and no attempt is made to compensate for any detector-to-detector photoresponse non-uniformity. Response correction is accomplished either in the on-board or ground signal processing by using dark data samples taken with the instrument shutter closed (to calibrate the offset for each array element) and calibration samples obtained while viewing the photometric calibration target or the inflight calibration lamp (to provide gain calibration data for each array element).

Digital Electronics. The required interface logic and microprocessor hardware is expected to be very similar to that for the CRAF TIR instrument. The sample processing and data handling is significantly different because of the much higher raw data rates and larger number of detectors for the SPP. Unlike the TIR, the microprocessor requires more logic external to the microprocessor to prevent the machine from being overloaded by interrupts occurring at the burst sample rate. The solution planned is the insertion of a small buffer memory between the ADC and the microprocessor so that interrupts occur less frequently, i.e., only when the buffer memory is full. Several other solutions are equally valid and some depend upon the availability of peripheral controllers available to interface with the Cassini project-supplied microprocessor. Selection of the optimal hardware/software approach for the SPP must await detailed definition of the CDS interface and microprocessor selection.

The instrument exchanges commands and data via serial interfaces which are connected to the instrument microprocessor via the project supplied BIU. The BIU also receives real time interrupts (RTIs) for synchronization of the instrument to the spacecraft telemetry system. Command and spacecraft status data such as time broadcasts and platform status are processed by the microprocessor and included where appropriate in the instrument output data format.

Random access memory chips are expected to be project-supplied in 64K by 1 sections, so 16 chips will comprise a 64K × 16 memory. With 10K words reserved for the program usage, more than 800 seconds of full spectro-polarimetry data with parity and housekeeping can be stored (without data compression) and an additional 25 seconds can be stored in the three 8800-bit buffers in the BIU. Correspondingly, more than 250 seconds of photometry data with truncated 10-bit samples with parity and housekeeping can be stored (without data compression) in the RAM memory. Permanent program code resides in the 8K Read-Only Memory (ROM) where 2K is allocated for BIU control and up to 6K for instrument control and data formatting. When the instrument power is turned "on" the code is relocated to a tested portion of the random access memory where it can be run without modification, or run after modification by ground command. During instrument operation, the ROM is powered down. Parallel ports from the microprocessor are used to control the shutter, retarder motor and calibration lamp via power drivers.

Discrete CMOS timing logic generates the clocks for the multiplexed arrays, controls signals for the analog electronics and multiplexer, and also controls the A/D converter and buffer memory. This logic includes a crystal oscillator providing the time base for the instrument. Since all of the high speed logic is performed without the use of the processor, much of its power can be applied to processing science data in order to minimize the telemetry data rate. For polarimetry measurements this includes the capability to apply gain and offset calibration factors to

each measurement. Such calibration factors are obtained from the inflight calibration sequences or from parameters uploaded from the ground (with default values being stored in ROM). Using calibrated measurements, the on-board calculation of scene polarization (magnitude and azimuth) provides one means to reduce the telemetry rate. Spectral editing either by selected spectral aggregation (which allows improved SNR at the expense of spectral resolution) or by deleting spectral data of the least importance for the particular scene being viewed are other approaches that can be used to tailor the SPP telemetry rate. Spectral normalization provides a simple means to reduce the raw 14-bit dynamic range (required since all array element gains are the same while scene spectral radiances and SPP responsivity varies with wavelength) to 12 bits. This normalization is equivalent to multiplication by ×1, ×2, or ×4 (as defined by ROM-resident selections or by ground uploads) followed by dropping the two least significant bits.

For photometry measurements the effective rate with data compression will be strongly dependent on the information content of the data. As suggested by the command parameters for photometry, a wide range of data rates can result, e.g., selection of the ×1024 aggregation as would be suitable for zodiacal light measurements reduces the data rate by the same factor. Similarly, the time windowed and event-threshold-windowed selections can allow substantial reductions of telemetered data with small or negligible loss of essential data during the limb and ring measurements. Due to the much lower SNR for the key limb, ring, and zodiacal light data than is warranted by the raw 14-bit quantization, simple data block renormalization and truncation to either 9 or 10 bits can be used to reduce data rate.

Power Conversion. It is anticipated that the power supply and BIU portion of the SPP electronics can be identical to that used on the CRAF TIR, based on the stated Cassini Project goal of CDS/PPS commonality for the two spacecraft. Instrument power is supplied by a balanced ±15 vdc bus with slow turn-on and current limiting to minimize in-rush current. Two small transformer coupled inverters are operated at 50 kHz and synchronized to the PPS sync signal. One inverter supplies the regulated electronic voltages and the second operates the retarder actuator, calibration lamp, and shutter actuator. Separating the inverters helps isolate the effects of motor pulses from the low level analog circuitry. The estimated SPP power breakdown is given in Table 3-6. Since the indicated pulsed loads are operated at very low duty cycles, they contribute little to the total average instrument power. The listed powers are validated from the actual conversion efficiencies and circuit performance of the PPR instrument.

Table 3-6. Estimated SPP Power.

Steady State Power		
Analog Electronics (includ. 75% conversion efficiency)	2.24W	
Digital Electronics (includ. 80% conversion efficiency)	1.50W	
BIU Electronics (includ. 80% conversion efficiency)	0.94W	
Total Power without Pulsed Loads	4.68W	
Total Average Pulsed Power for typical (and worst case) duty cycles		
Calibration Lamp @ 0.60 W with < 1% (5%) duty cycle	0.01W	(0.03W)
Shutter Actuator @ 0.05 W with 2% (50%) duty cycle	0.001W	(0.03W)
Retarder Actuator @ 4.50 W with 2% (16%) duty cycle	0.09W	(0.72W)
Averaged Pulsed Power (Worst Case Duty Cycle)	0.10W	(0.78W)
Summary		
Average Power for Typical (and worst case) duty cycles	4.8W	(5.5W)
Peak Power (Note: BIU and actuator pulsed loads not coincident)	9.2W	
Replacement Heater Power (with SPP power off)	2.5W	